Electronic Supplementary Material (ESI) for RSC Advances.

Supporting Information for

A Novel 3D Terbium Metal-Organic Framework as a Heterogeneous Lewis Acid Catalyst for the Cyanosilylation of Aldehyde

Yuqian Liu, Peiran Zhao, Chunying Duan, and Cheng He*

Dalian University of Technology, State Key Laboratory of Fine Chemicals, Dalian 116012, P. R. China. Corresponding author e-mail address: hecheng@dlut.edu.cn

^{1}H NMR spectral data of H_2sbdc.
(500 Mhz, DMSO-d_6): d = 8.53 (d, J = 8.0 Hz, 2H), 8.50 (S, 2H), 8.46 (d, J = 8.0 2H).[1]

^{1}H NMR spectral data TMSCN.
(500 MHz, $CDCl_3$): δ 0.30 (9H, s, $SiCH_3$).

^{1}H NMR spectral data 1,3,5-Trimethoxybenzene.
(500 MHz, $CDCl_3$): δ 3.78 (9H, s, OCH_3), 6.10 (3H, s, ArH).[2]

^{1}H NMR spectral data of different aldehydes.
2-Nitobenzaldehyde (400 MHz, $CDCl_3$): δ 10.40 (s, 1H, CHO), 8.10 (dd, *J* = 7.6, 1.6 Hz, 1H, Ar-CH), 7.90 (dd, *J* = 7.2, 1.6 Hz, 1H, Ar-CH), 7.80-7.70 (m, 2H, Ar-CH).[3]
3-Nitobenzaldehyde (400 MHz, $CDCl_3$) δ 10.12 (s, 1H), 8.71 (dd, *J* = 2.3, 1.6 Hz, 1H), 8.50-8.47 (m, 1H), 8.25-8.22 (m, 1H), 7.79-7.75 (m, 1H).[4]
4-Nitobenzaldehyde (400 MHz, $CDCl_3$): δ 10.18 (s, 1H, CHO), 8.41 (d, *J* = 8.0 Hz, 2H, Ar-CH), 8.10 (d, *J* = 8.0 Hz, 2 H, Ar-CH).[3]
2-Naphthaldehyde (400 MHz, $CDCl_3$) δ 10.37 (s, 1H), 9.26 (d, *J* = 8.7 Hz, 1H), 8.06 (d, *J* = 8.2 Hz, 1H), 7.94 (dd, *J* = 7.1, 1.2 Hz, 1H), 7.89 (d, *J* = 8.2 Hz, 1H), 7.70-7.65 (m, 1H), 7.61-7.55 (m, 2H).[5]
***o*-Methoxybenzaldehyde** (500 MHz, $CDCl_3$) δ 10.45 (s, 1H), 7.82-7.80 (dd, 1H, *J* = 9.6, 2.3 Hz), 7.56-7.51 (ddd, 1H, *J* = 10.6, 9.2, 2.3 Hz), 7.03-6.96 (m, 2H), 3.91 (s, 3H).[6]
***m*-Methoxybenzaldehyde** (400 MHz, $CDCl_3$) δ 9.94 (s, 1H), 7.45-7.38 (m, 2H), 7.36 (d, *J* = 1.9 Hz, 1H), 7.16-7.13 (m, 1H), 3.83 (s, 3H).[5]
***p*-Methoxybenzaldehyde** (400 MHz, $CDCl_3$): δ 9.83 (s, 1H, CHO), 8.17-7.55 (m, 2H, Ar-CH), 6.59 (d, *J* = 8.7Hz, 2H, Ar-CH), 3.83 (m, 3H, OCH_3).[3]
Heptanal (400 MHz, $CDCl_3$) δ 9.74 (s, 1H), 2.38 (t, 2H), 1.63-1.57 (m, 2H), 1.39-1.21 (m, 6H), 0.90-0.83 (t, 3H).[7]
Salicylaldehyde (500 MHz, $CDCl_3$): δ 11.06 (s, 1H, -OH), 9.93 (s, 1H, -CHO), 7.60 (m, 1H, ArH), 7.56 (m, 1H, ArH), 7.07 (m, 1H, ArH), 7.03 (m, 1H, ArH).[8]
4-Biphenylcarboxaldehyde (500 MHz, $CDCl_3$): 7.40-7.52 (3H, m, H-Ar), 7.75 (2H, d, *J* = 7.6 Hz, H-Ar), 7.86 (2H, d, *J* = 6.8 Hz, H-Ar), 7.98 (2H, d, *J* = 6.8 Hz, H-Ar), 10.05 (1H, s, CHO).[9]
4-(Diethylamino)salicylaldehyde (400 MHz, $CDCl_3$): δ 11.65 (br, 1H), 9.49 (s, 1H), 7.27 (d, *J* = 8.8 Hz, 1H), 6.27 (d, *J* = 10.2 Hz, 1H), 6.08 (s, 1H), 3.41 (q, *J* = 7.0 Hz, 4H), 1.22 (t, *J* = 7.1 Hz, 6H).[10]
4-Benzyloxybenzaldehyde (400 MHz; $CDCl_3$) 5.15 (2H, s, $PhCH_2$), 7.08 (2H, d, *J* = 8.7 Hz, ArH), 7.34-7.47 (5H, m, ArH overlapping), 7.84 (2H, d, *J* = 8.8 Hz, ArH) and 9.89 (1H, s, HC=O).[11]

^{1}H NMR spectral data of the product of different aldehydes in cyanosilylation.
The product of 2-Nitobenzaldehyde ^{1}H-NMR (500 MHz, $CDCl_3$): δ 8.18-8.20 (d, 1H, *J* = 8.20 Hz), 7.97-7.99 (d, 1H, *J* = 8.20 Hz), 7.78-7.82 (t, 1H, *J* = 7.80 Hz),

7.63-7.66 (t, 1H, *J* = 7.80 Hz), 6.20 (s, 1H), 0.07 (s, 9H).[12]

The product of 3-Nitobenzaldehyde (300 MHz, $CDCl_3$): δ 0.29 (s, 9H, $Si(CH_3)_3$), 5.60 (s, 1H, $CHOSi(CH_3)_3$), 7.63 (t, *J* = 4.5 Hz, 1H, Ph), 7.84 (d, J = 6.0 Hz, 1H, Ph), 8.26 (d, J = 8.0 Hz, 1H, Ph) , 8.34 (s,1H, Ph).[13]

The product of 4-Nitobenzaldehyde (600 MHz, $CDCl_3$): δ 0.29 (s, 9 H, $Si(CH_3)_3$), 5.64 (s, 1 H, OCHCN), 6.68 (d, *J* = 8.4 Hz, 2 H, ArH), 8.28 (d, *J* = 8.4 Hz, 2 H, ArH).[14]

The product of 2-Naphthaldehyde (200 MHz, $CDCl_3$): δ 0.11 (s, 9H, $Si(CH_3)_3$, 5.95 (s, 1H, $CHOSi(CH_3)_3$), 7.37-7.63(m, 4H, Ph), 7.78(d, *J*= 7.5 Hz, 2H, Ph), 8.07(d, *J*= 8.0 Hz, 1H, Ph).[15]

The product of *o*-Methoxybenzaldehyde (300 MHz, $CDCl_3$) δ 7.62-7.58 (m, 1 H), 7.40-7.33 (m, 1 H), 7.08-6.98 (m, 1 H), 6.94-6.86 (m, 1 H), 5.81 (s, 1 H), 3.89 (s, 3 H), 0.41-0.14 (m, 9 H).[16]

The product of *m*-Methoxybenzaldehyde (400 MHz, $CDCl_3$): δ 7.32 (t, 1H, J = 7.9 Hz, aromatics), 7.05-7.02 (m, 2H, aromatics), 6.92 (dd, 1H, J = 8.2, 2.0 Hz aromatic), 5.47 (s, 1H, CHCN), 3.83 (s, 3H, CH_3O), 0.24 (s, 9H, $Si(CH_3)_3$).[17]

The product of *p*-Methoxybenzaldehyde (250 MHz, $CDCl_3$): δ 7.38 (d, 2H, *J* = 8.8 Hz, Ph-2H, 6H), 6.92 (d, 2H, *J* = 8.8 Hz, Ph-3H, 5H), 5.43 (s, 1H, CH), 3.82 (s, 3H, OCH_3), 0.21 (s, 9H, $(CH_3)_3$).[18]

The product of Heptanal (400 MHz, $CDCl_3$): δ 0.20(9H, s), 0.89(3H, t), 1.25-1.36(6H, m), 1.40-1.48(2H, m), 1.75-1.81(2H, m), 4.38(1H, t).[19]

The product of Salicylaldehydeδ 11.50 (br, 1H), 7.62-7.58 (m, 1H), 7.40-7.33 (m, 1H), 7.08-6.98 (m, 1H), 6.94-6.86 (m, 1H), 5.57 (s, 1H), 0.22(s, 9H).[20]

The product of 4-Biphenylcarboxaldehyde (400 MHz, $CDCl_3$): δ 7.60−7.51 (m, 7H), 7.45−7.41 (m, 2H), 7.36−7.33 (m, 1H), 5.53 (s, 1H), 0.25 (s, 9H).[21]

The product of 4-(Diethylamino)salicylaldehyde (400 MHz, $CDCl_3$): δ 11.50 (br, 1H), 7.27 (d, *J* = 8.8 Hz, 1H), 6.27 (d, *J* = 10.2 Hz, 1H), 6.08 (s, 1H), 3.41 (q, *J* = 7.0 Hz, 4H), 1.22 (t, *J* = 7.1 Hz, 6H)， 0.25 (s, 9H).[22]

The product of 4-Benzyloxybenzaldehyde (200 MHz, $CDCl_3$): 0.22 (s, 9H), 5.46 (s, 1H), 6.99-7.13 (m, 5H), 7.31-7.44 (m, 4H).[23]

The method for calculating the conversion.

1,3,5-Trimethoxybenzene had 3 H protons on benzene ring (δ ppm = 6.10). All the product had 1 H proton on their chiral C proton. Consequently, the yield of the reactions could be read from the ^1H spectrum directly, as the same amount of 1,3,5-Trimethoxybenzene (compared to the aldehyde) was added into the system before monitoring the ^1H spectrum.

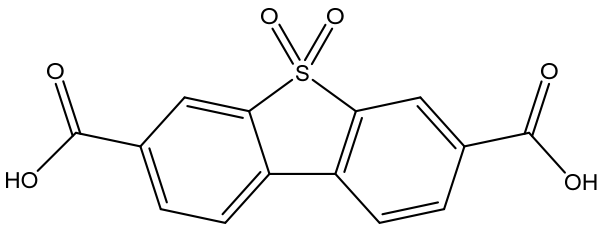

Fig. S1 Chemical structure of H_2sbdc.

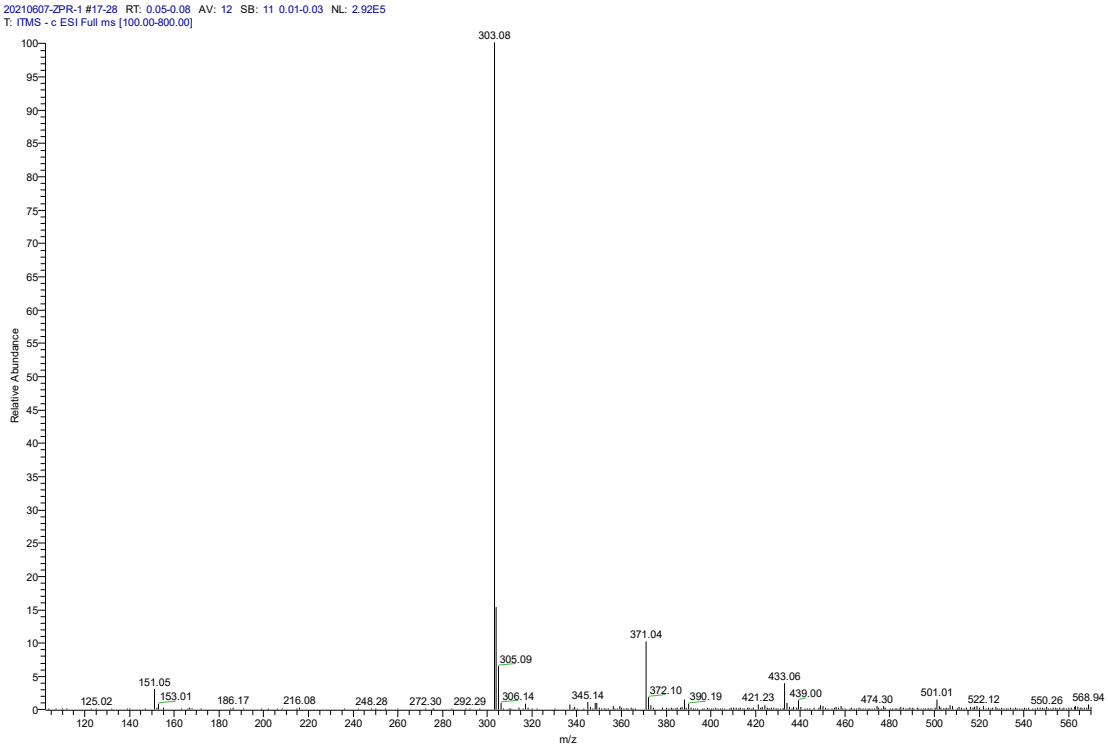

Fig. S2 MS for H_2sbdc.

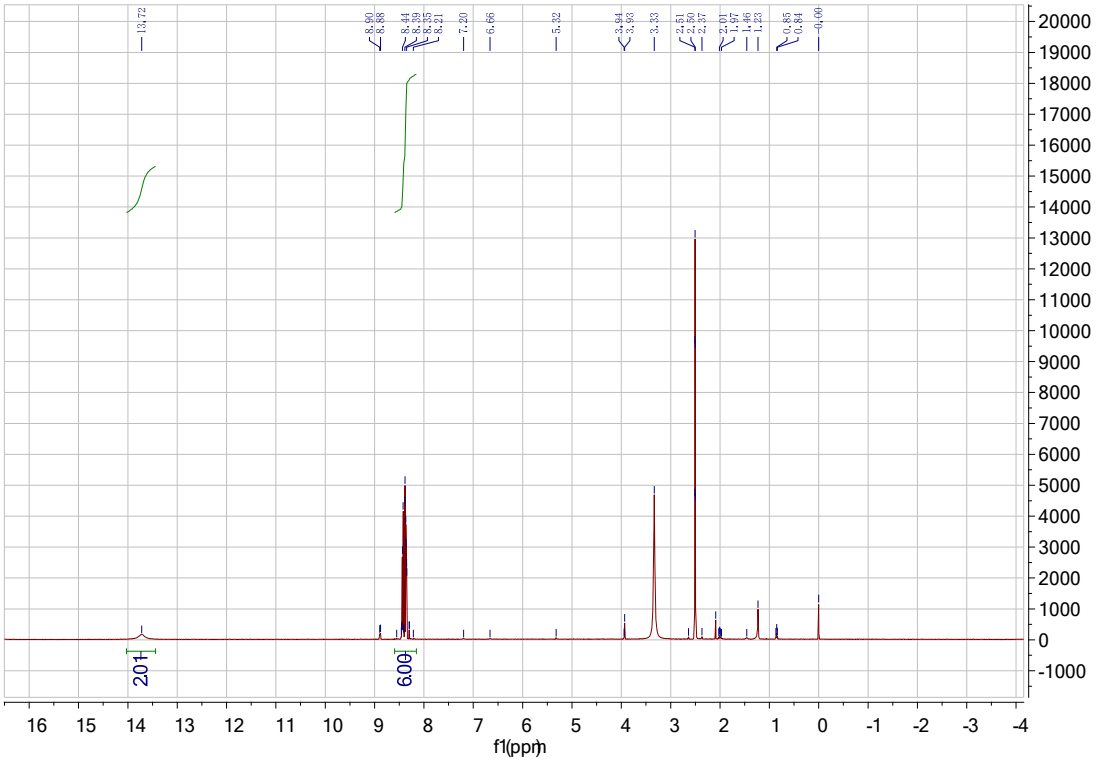

Fig. S3 ^{1}H-NMR for H_2sbdc.

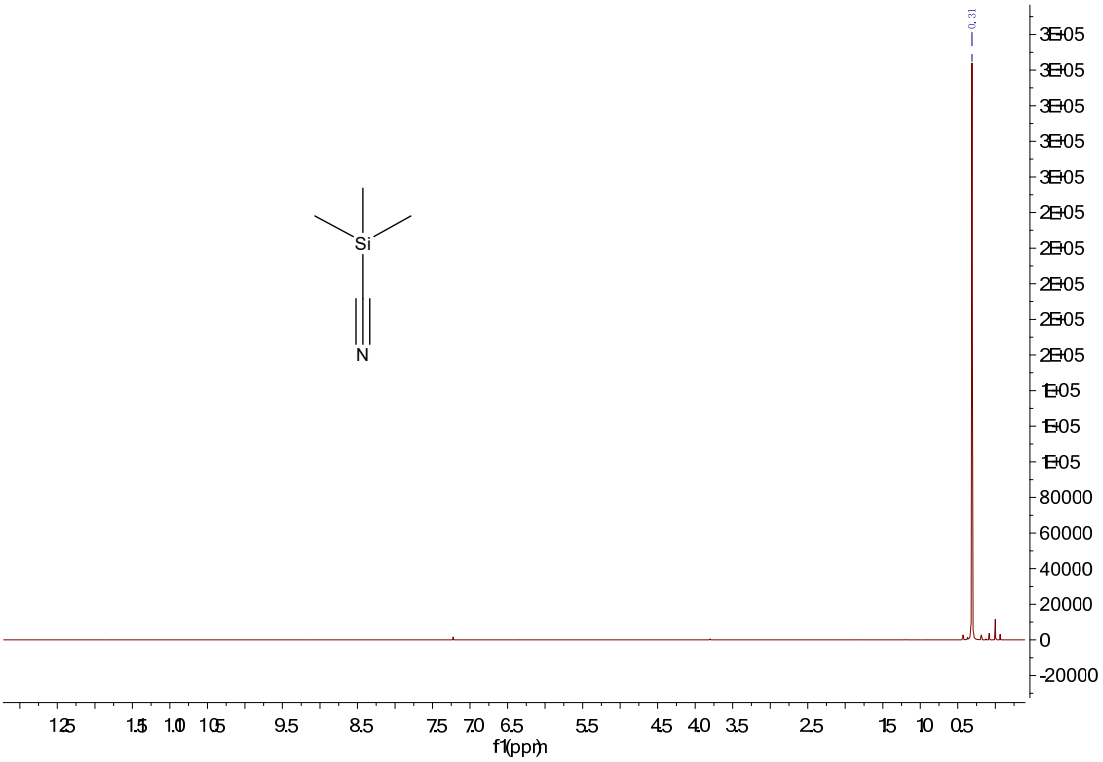

Fig. S4 ^{1}H-NMR for TMSCN.

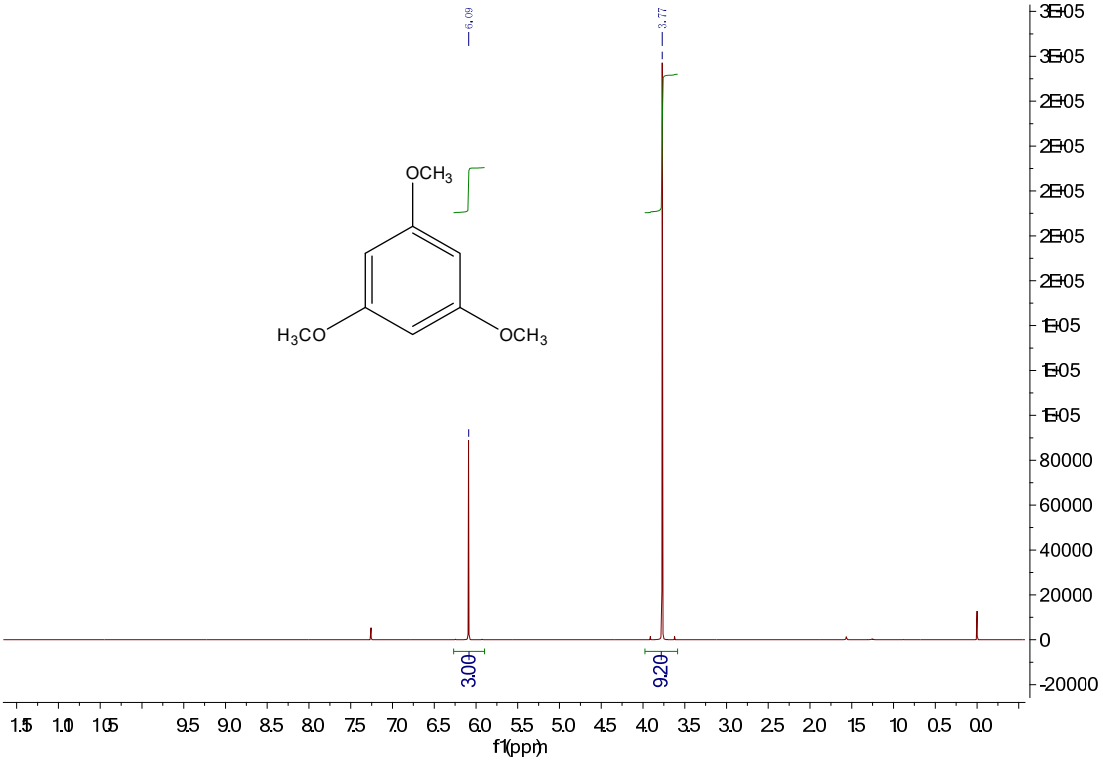

Fig. S5 ^{1}H-NMR for 1,3,5-Trimethoxybenzene.

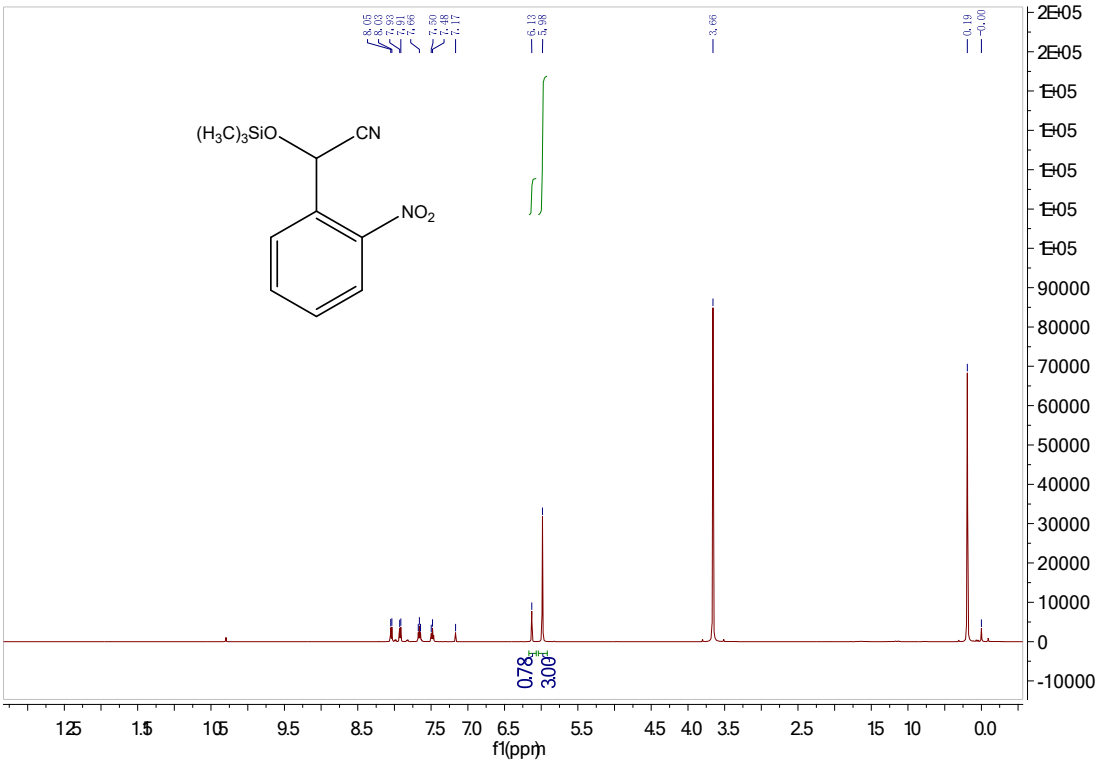

Fig. S6 ^{1}H-NMR for catalysis of 2-nitrobenzaldehyde 2.4 eqv TMSCN in DCM for 12h.

Yield = 78%

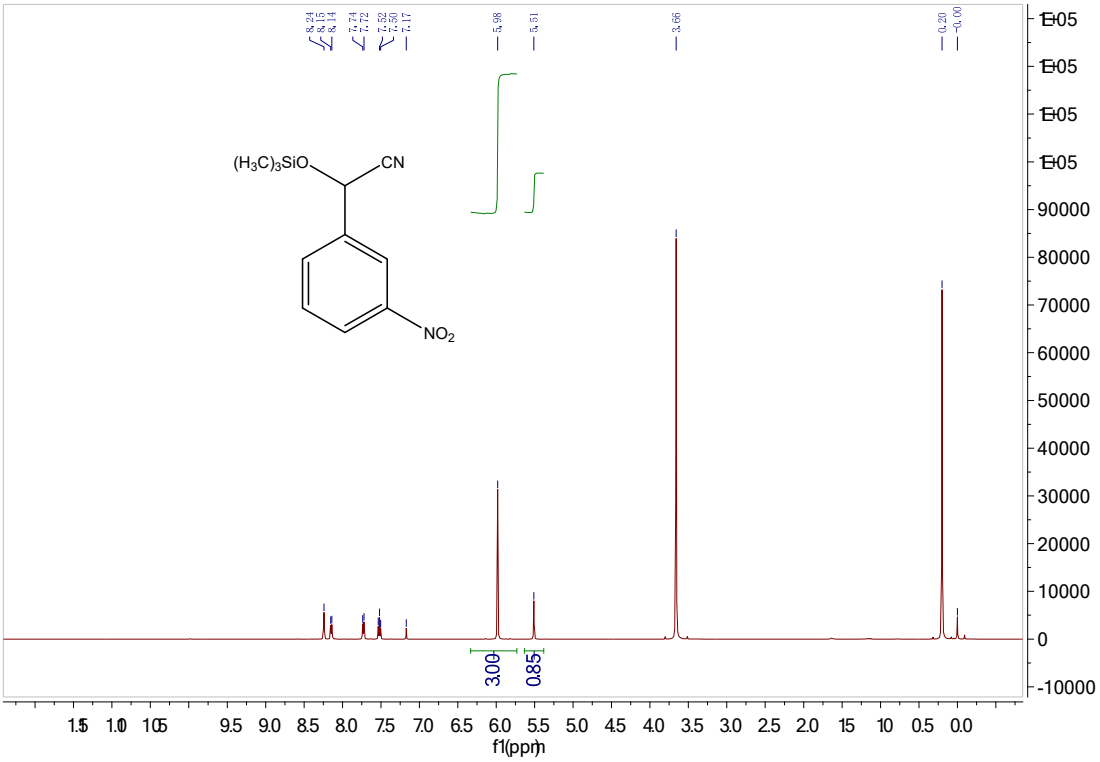

Fig. S7 ^{1}H-NMR for catalysis of 3-nitrobenzaldehyde 2.4 eqv TMSCN in DCM for 12h.

Yield = 85%

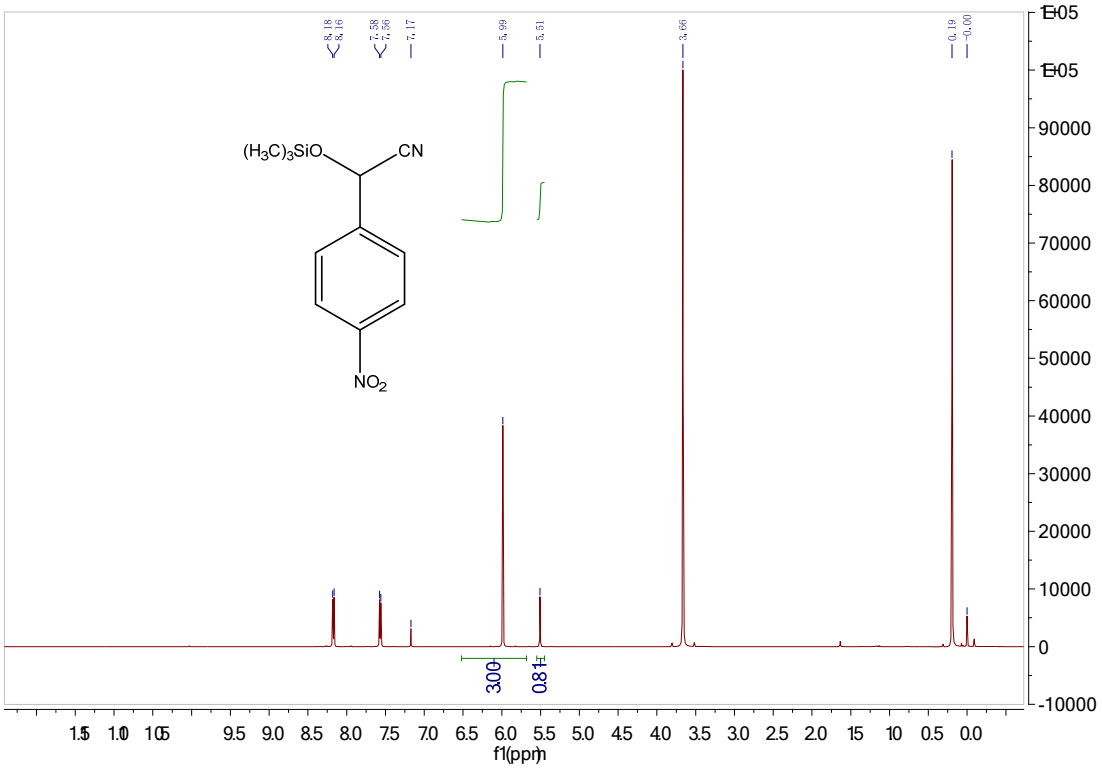

Fig. S8 ^{1}H-NMR for catalysis of 4-nitrobenzaldehyde 2.4 eqv TMSCN in DCM for 12h.
Yield = 81%

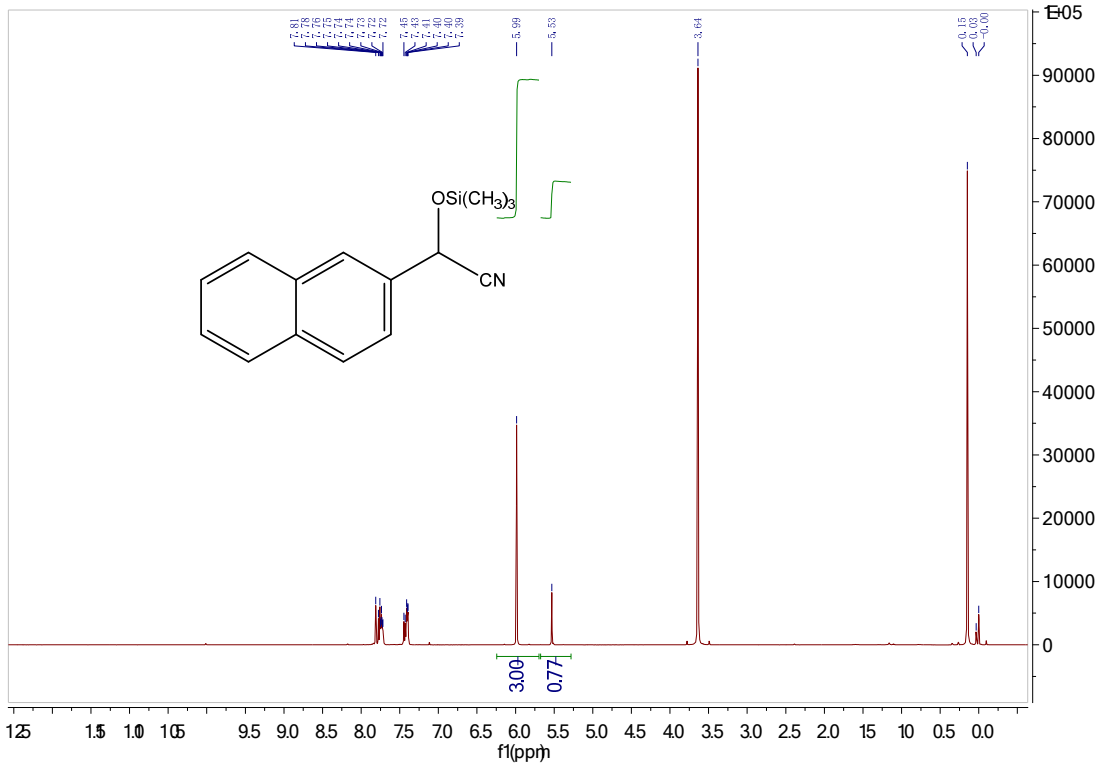

Fig. S9 ^{1}H-NMR for catalysis of 2-naphthaldehyde 2.4 eqv TMSCN in DCM for 12h.
Yield = 77%

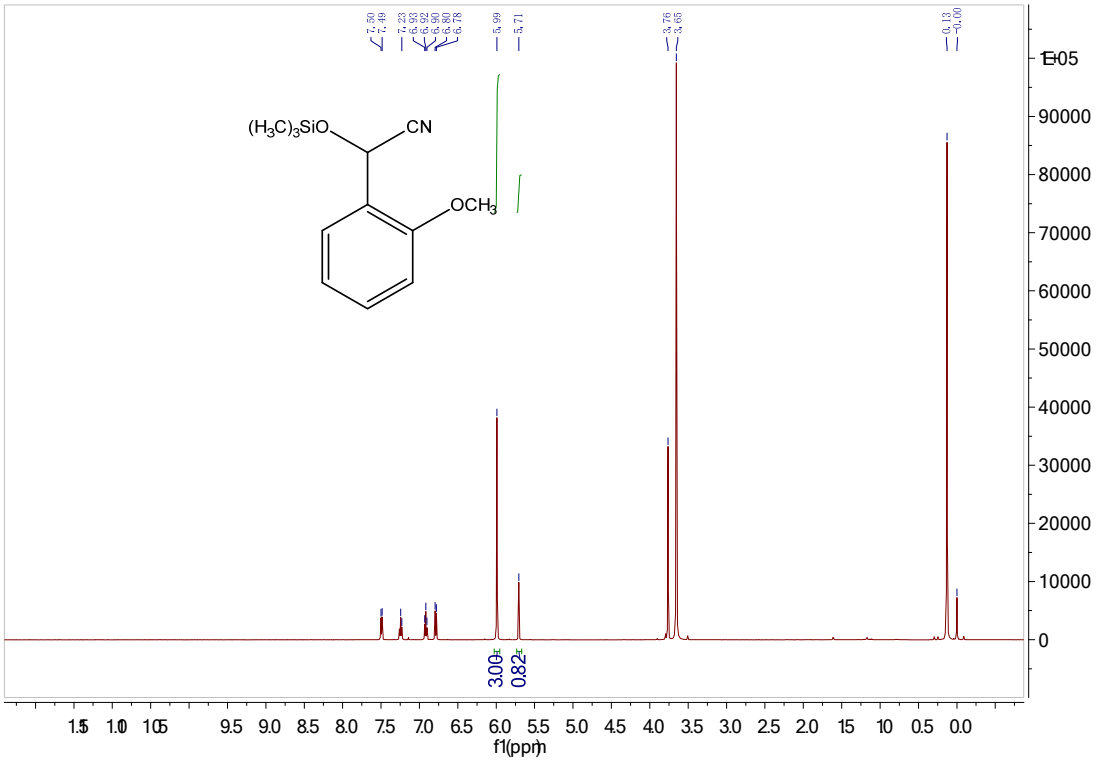

Fig. S10 ^{1}H-NMR for catalysis of 2-methoxybenzaldehyde 2.4 eqv TMSCN in DCM for 12h.
Yield = 82%

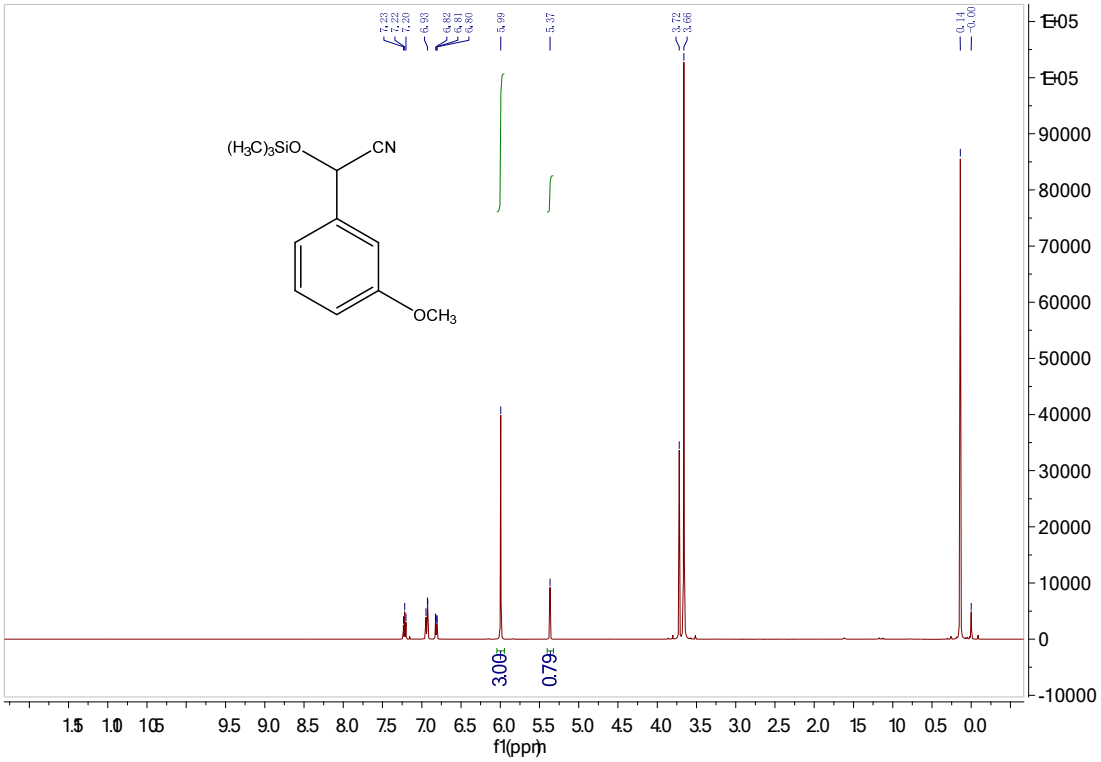

Fig. S11 ^{1}H-NMR for catalysis of 3-methoxybenzaldehyde 2.4 eqv TMSCN in DCM for 12h.
Yield = 79%

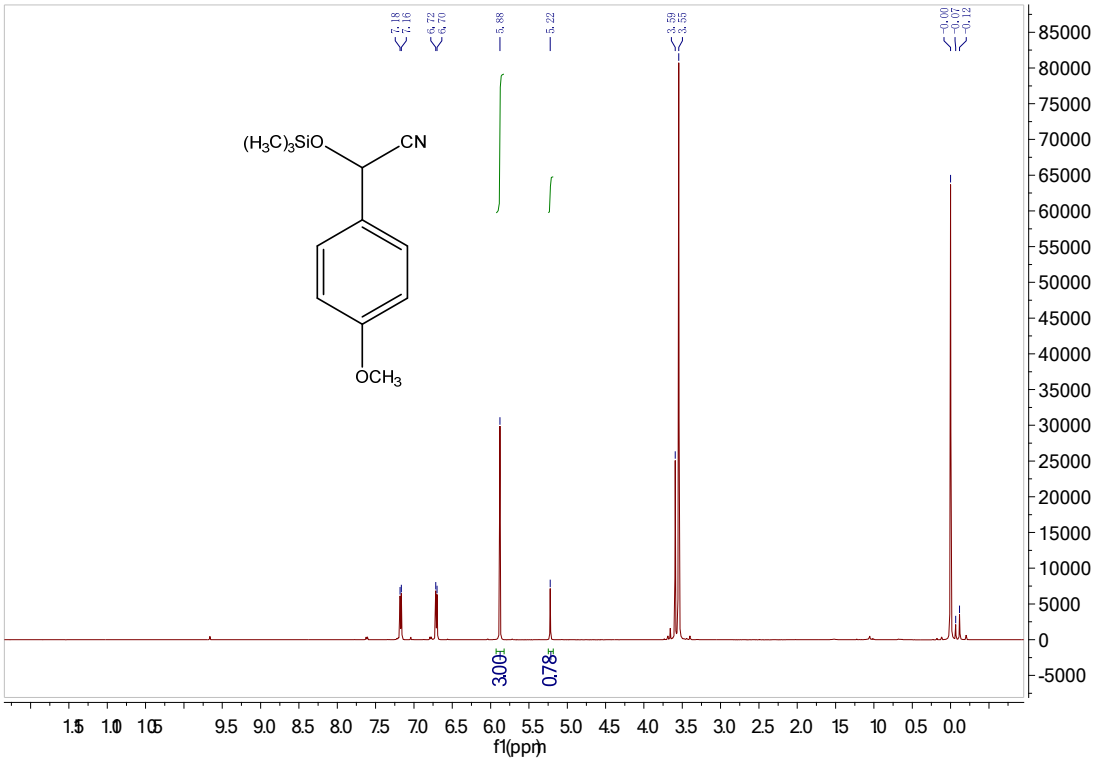

Fig. S12 ^{1}H-NMR for catalysis of 4-methoxybenzaldehyde 2.4 eqv TMSCN in DCM for 12h.
Yield = 78%

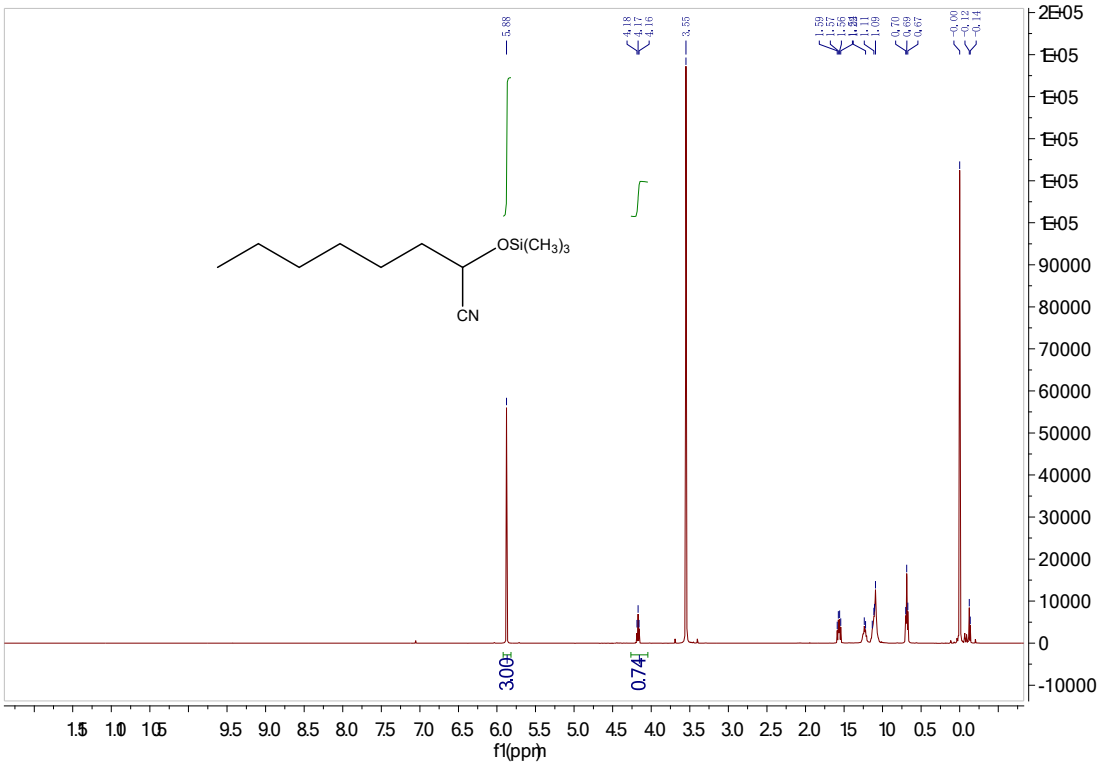

Fig. S13 ^{1}H-NMR for catalysis of heptanal 2.4 eqv TMSCN in DCM for 12h.
Yield = 74%

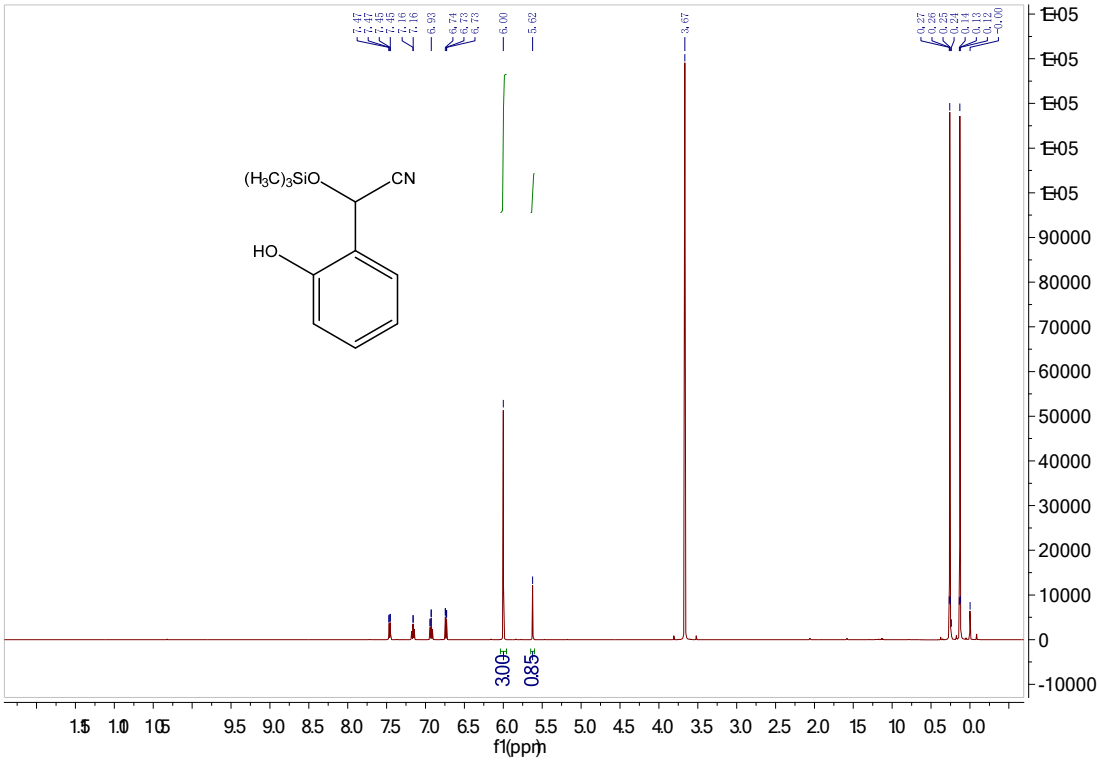

Fig. S14 ^{1}H-NMR for catalysis of salicylaldehyde 2.4 eqv TMSCN in DCM for 12h.
Yield = 85%

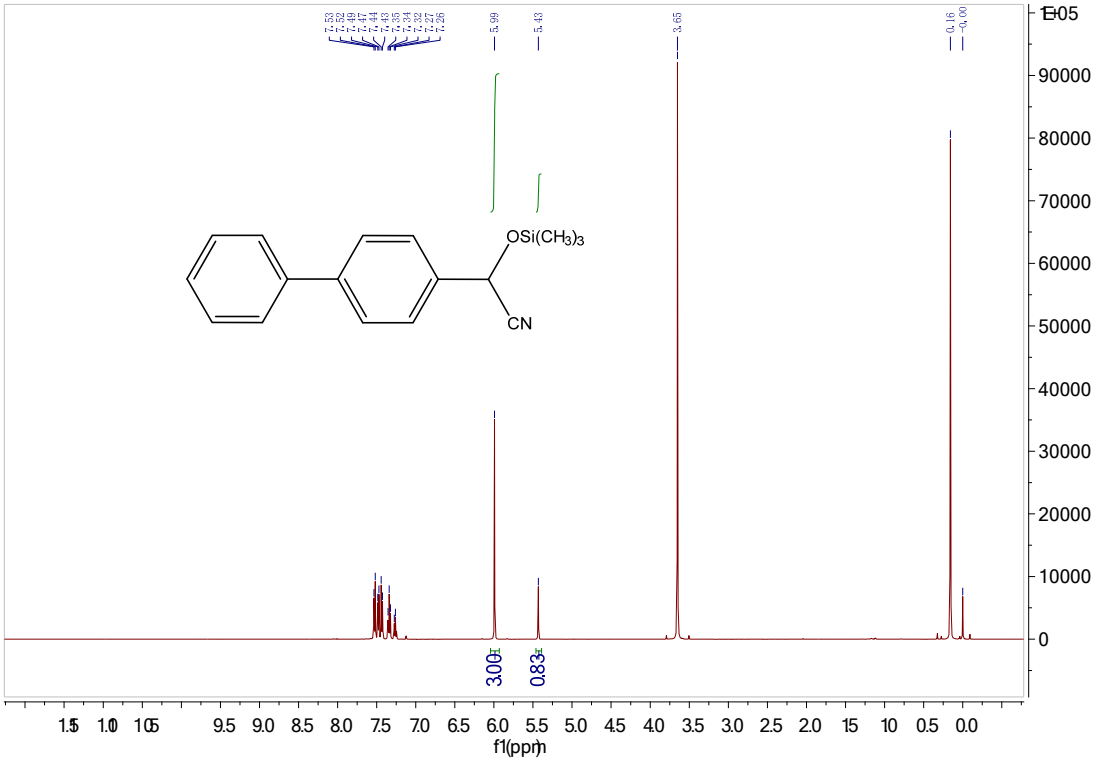

Fig. S15 ^{1}H-NMR for catalysis of 4-Biphenylcarboxaldehyde 2.4 eqv TMSCN in DCM for 12h.
Yield = 83%

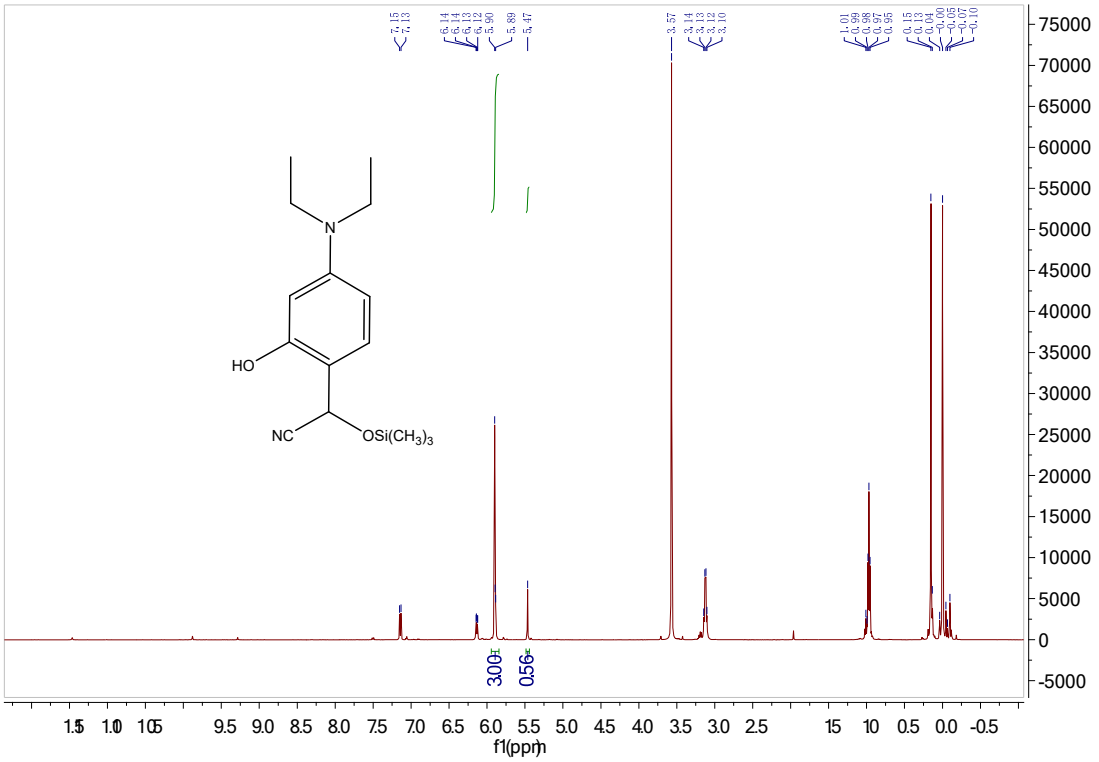

Fig. S16 ^{1}H-NMR for catalysis of 4-(diethylamino)salicylaldehyde 2.4 eqv TMSCN in DCM for 12h.
Yield = 56%

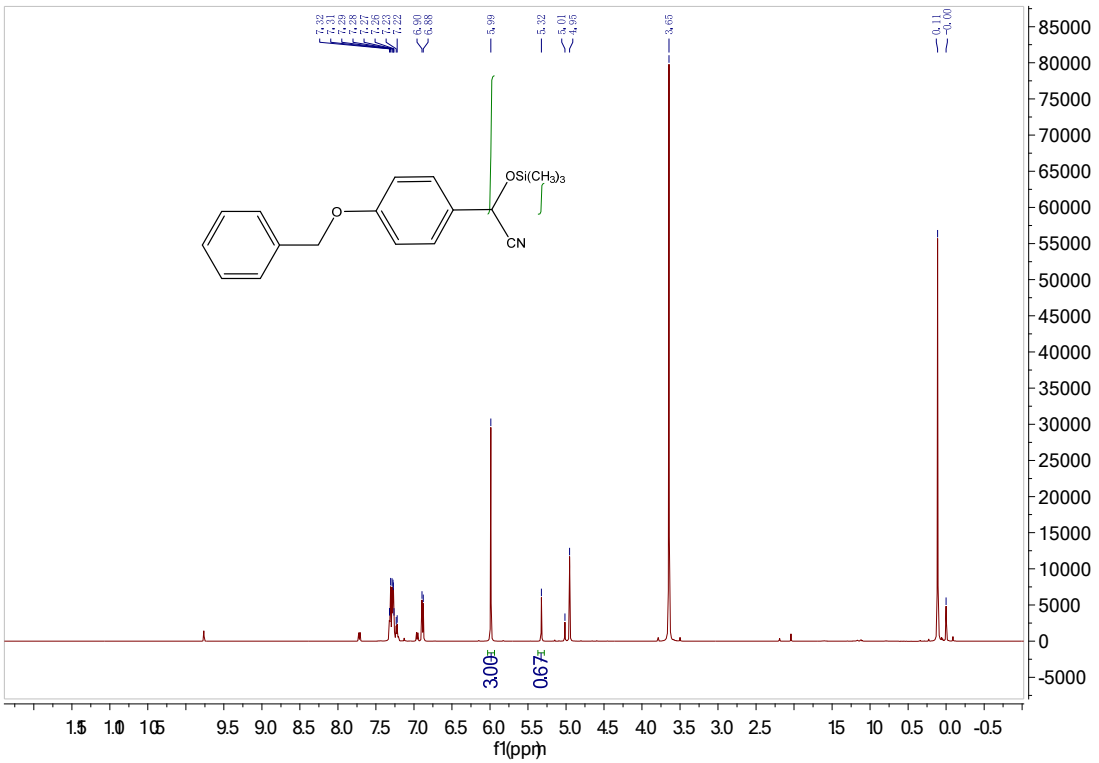

Fig. S17 ^{1}H-NMR for catalysis of 4-benzyloxybenzaldehyde 2.4 eqv TMSCN in DCM for 12h.
Yield = 67%

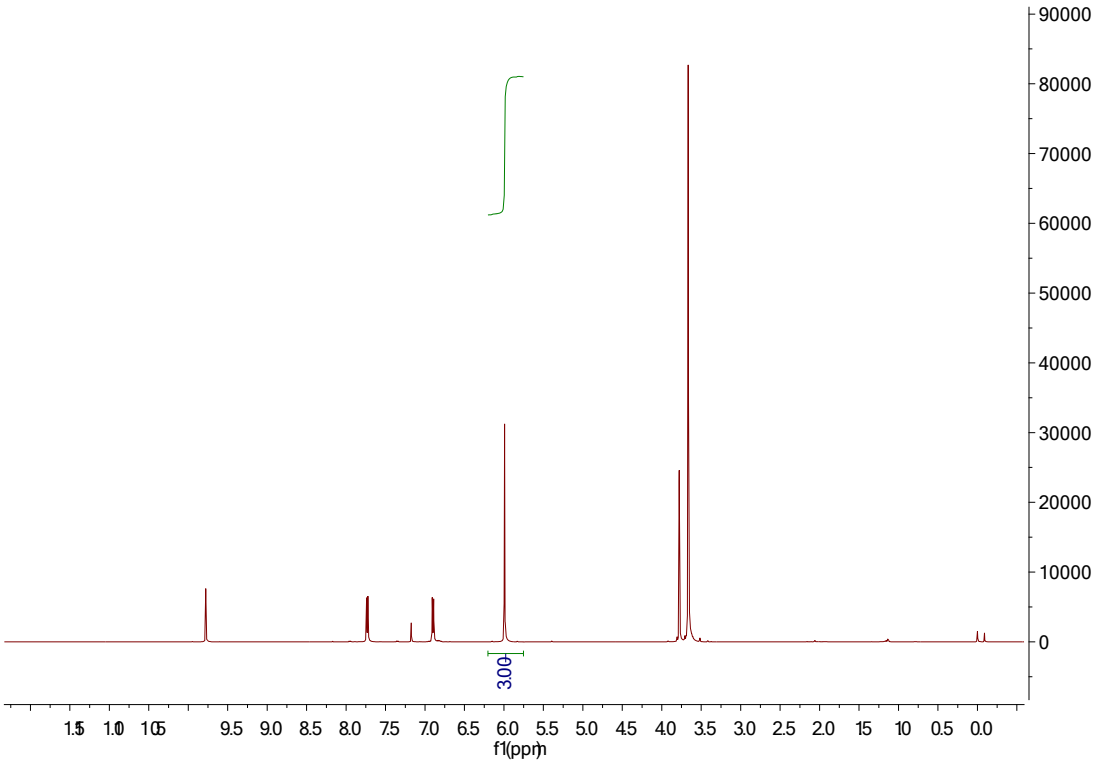

Fig. S18 ^{1}H-NMR for catalysis of 4-methoxybenzaldehyde 2.4 eqv TMSCN in EtOH for 12h.
Yield = 0%

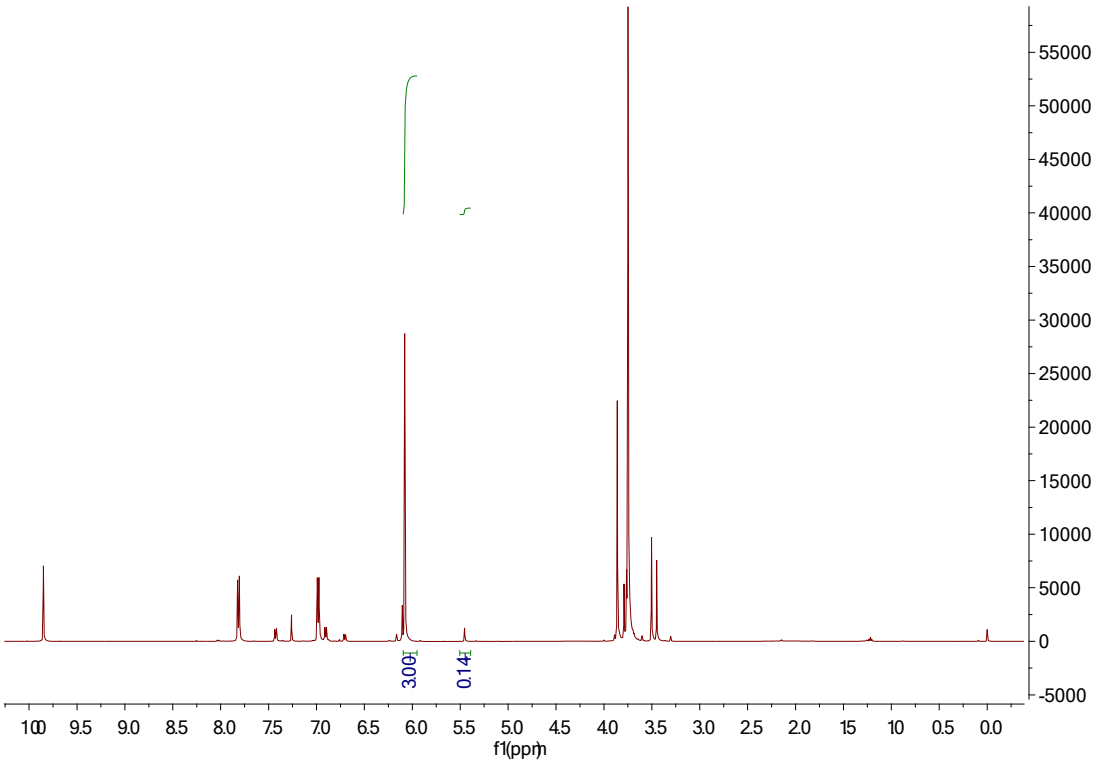

Fig. S19 ^{1}H-NMR for catalysis of 4-methoxybenzaldehyde 2.4 eqv TMSCN in MeOH for 12h.
Yield = 14%

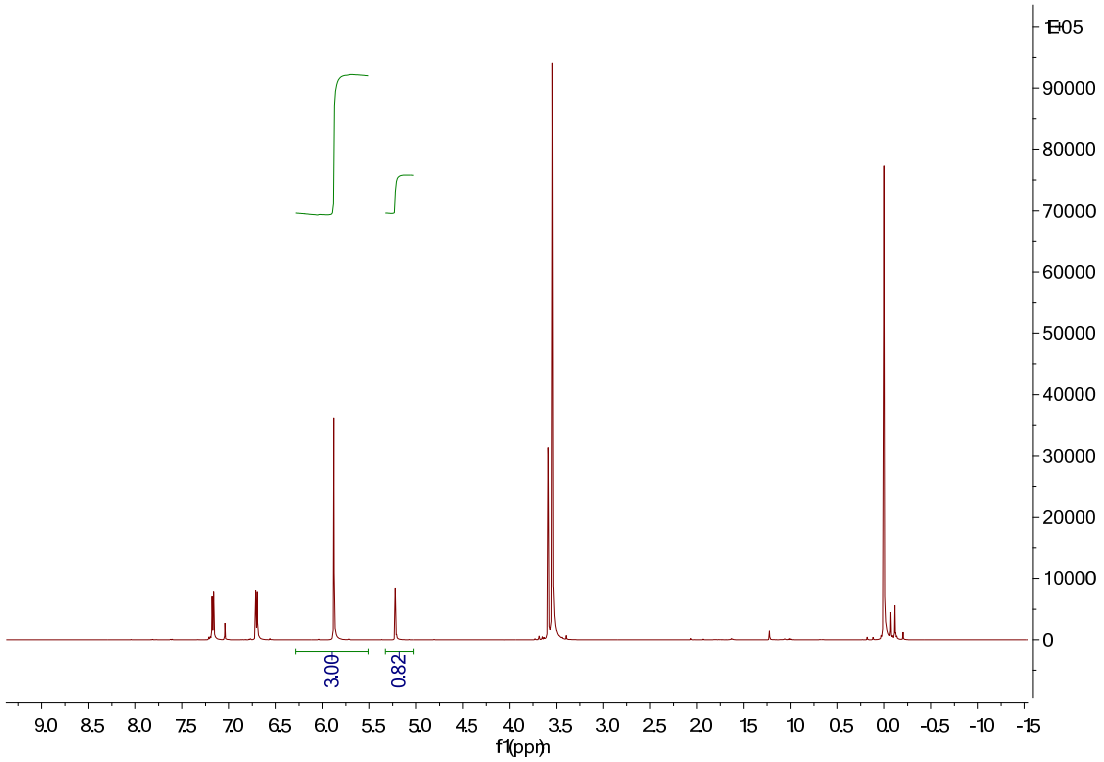

Fig. S20 ^{1}H-NMR for catalysis of 4-methoxybenzaldehyde 2.4 eqv TMSCN in THF for 12h.
Yield = 82%

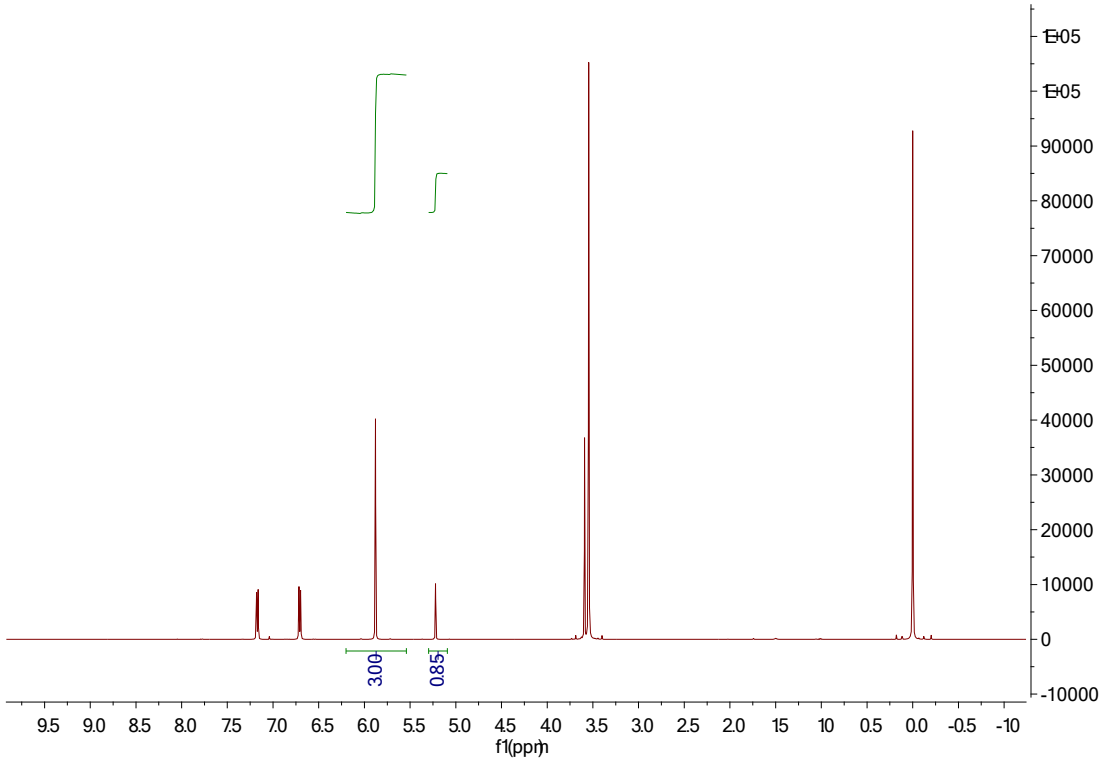

Fig. S21 ^{1}H-NMR for catalysis of 4-methoxybenzaldehyde 2.4 eqv TMSCN in CH_3CN for 12h.
Yield = 85%

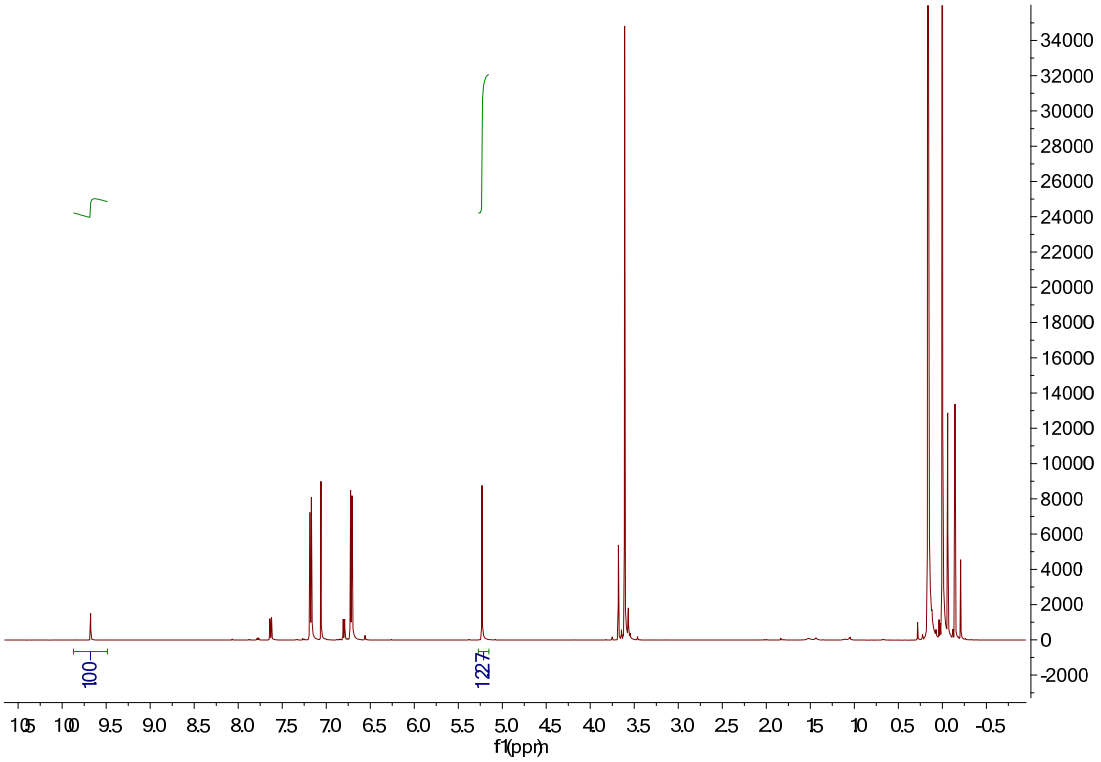

Fig. S22 ^{1}H-NMR for catalysis of 4-methoxybenzaldehyde with 2.4 eqv TMSCN in solvent free condition for 12h.
Yield = 12.27/(1+12.27) = 92%

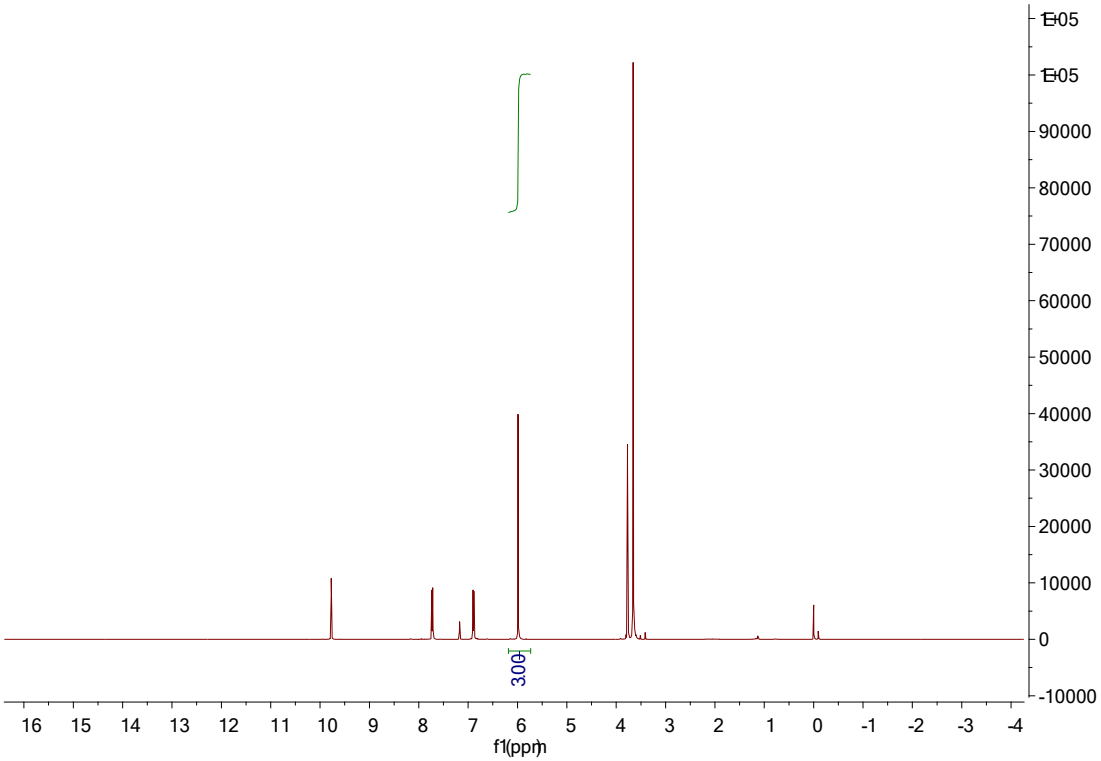

Fig. S23 ^{1}H-NMR for catalysis of 4-methoxybenzaldehyde in DCM with 0 eqv TMSCN for 12h.
Yield = 0%

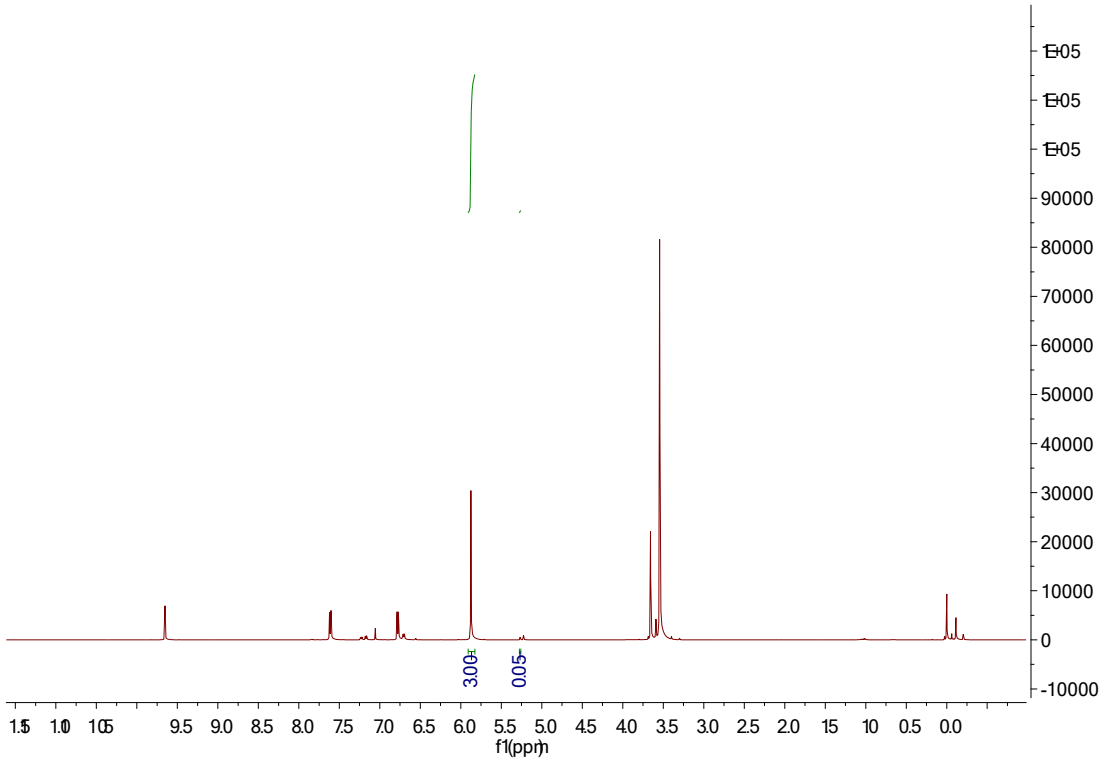

Fig. S24 ^{1}H-NMR for catalysis of 4-methoxybenzaldehyde in DCM with 0.5 eqv TMSCN for 12h.
Yield = 5%

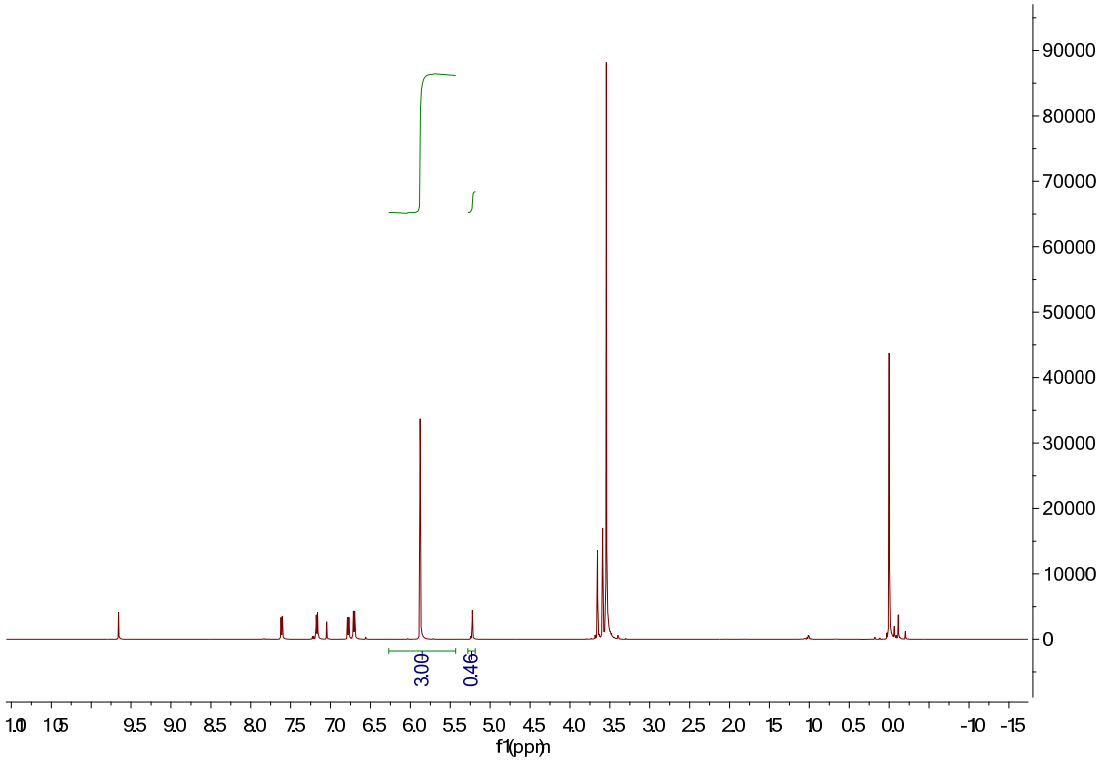

Fig. S25 ^{1}H-NMR for catalysis of 4-methoxybenzaldehyde in DCM with 1 eqv TMSCN for 12h.
Yield = 46%

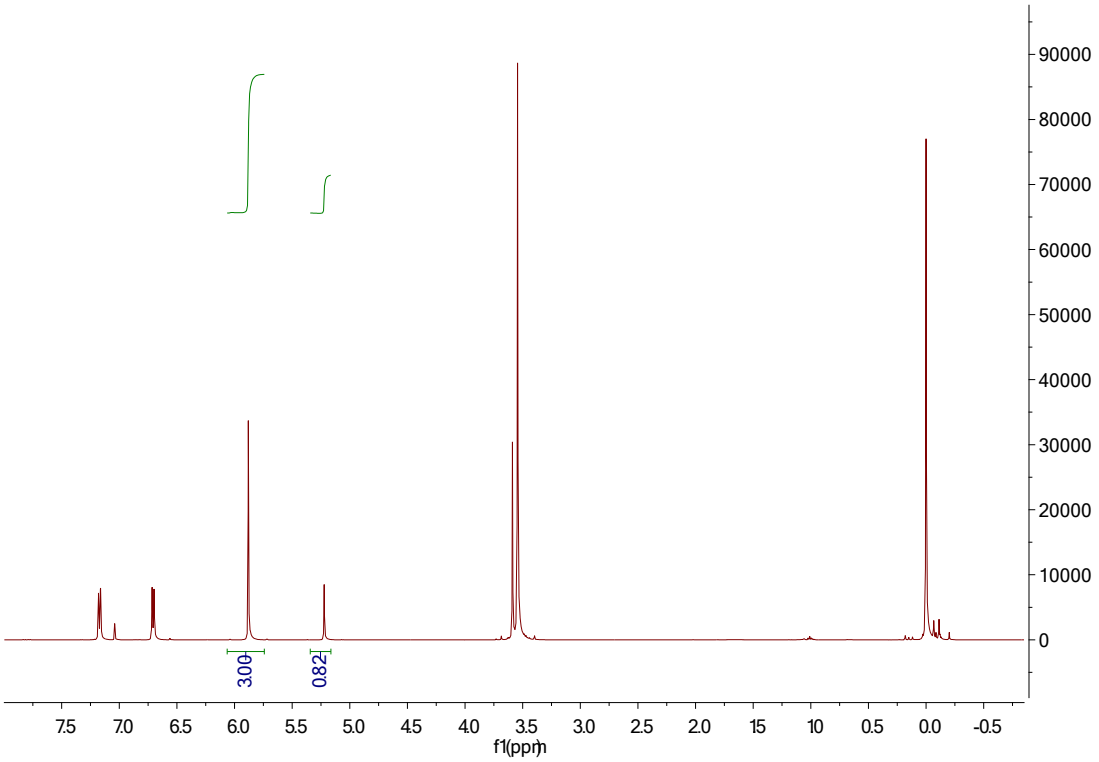

Fig. S26 ^{1}H-NMR for catalysis of 4-methoxybenzaldehyde in DCM with 3 eqv TMSCN for 12h.
Yield = 82%

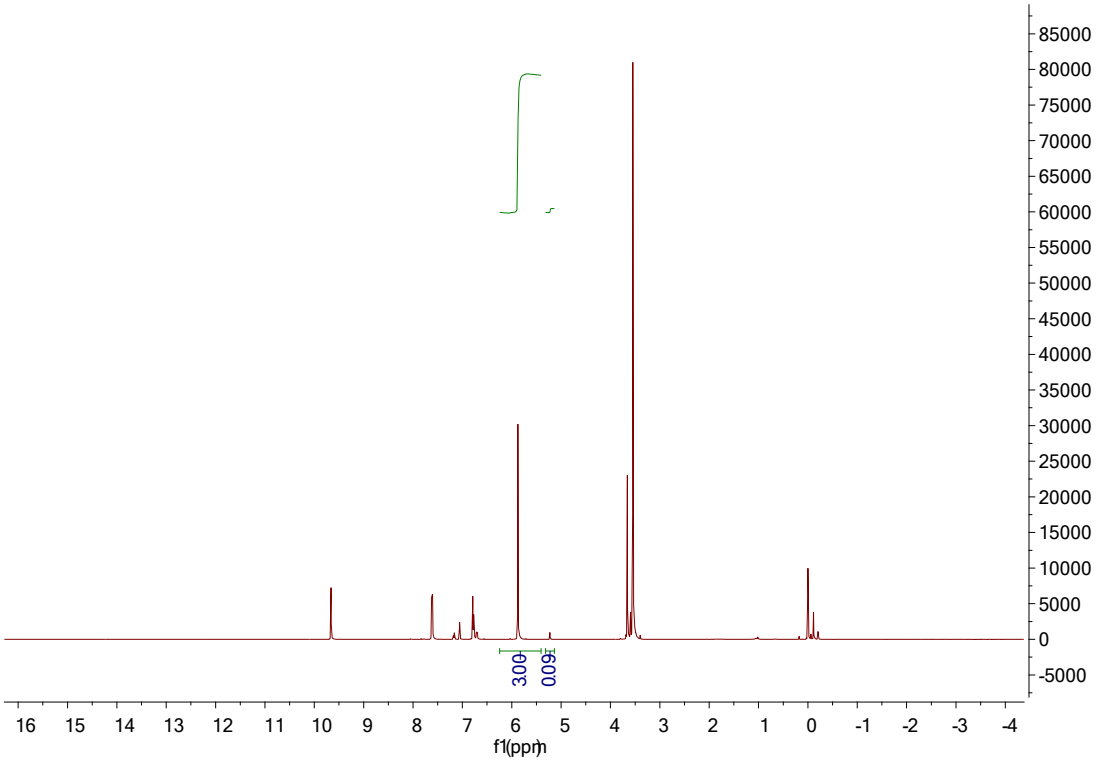

Fig. S27 ^{1}H-NMR for catalysis of 4-methoxybenzaldehyde in DCM with 2.4 eqv TMSCN for 1h.
Yiled = 9%

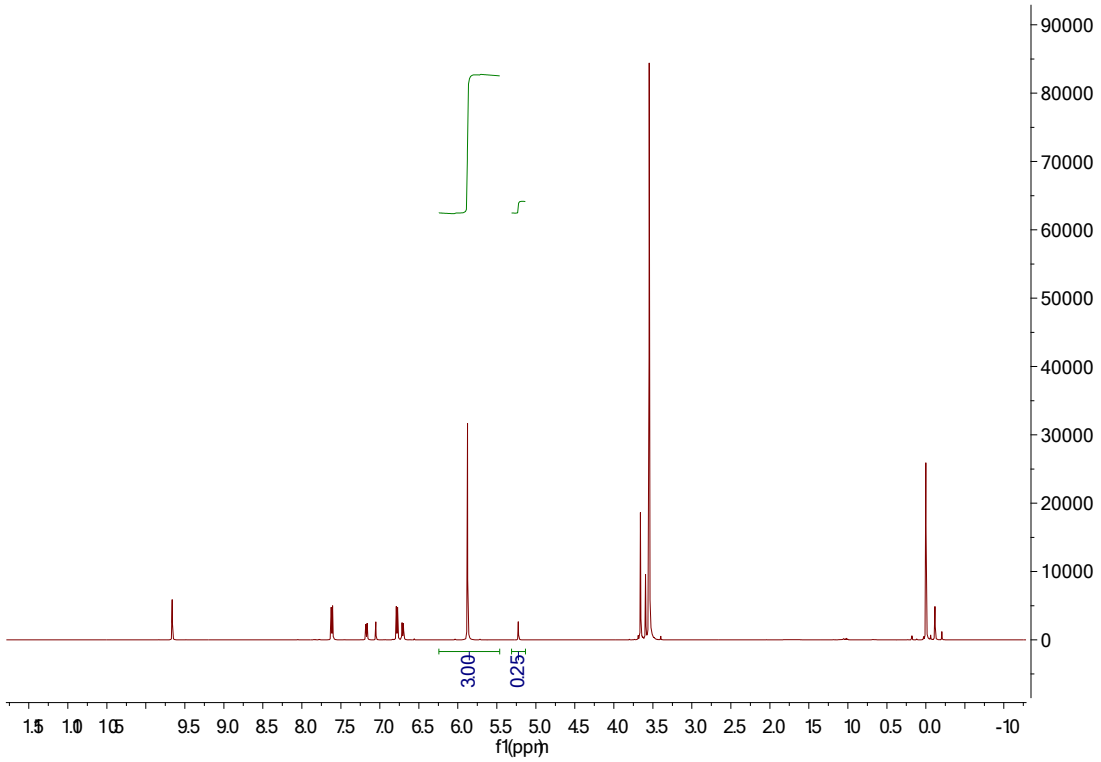

Fig. S28 ^{1}H-NMR for catalysis of 4-methoxybenzaldehyde in DCM with 2.4 eqv TMSCN for 2h.
Yiled = 25%

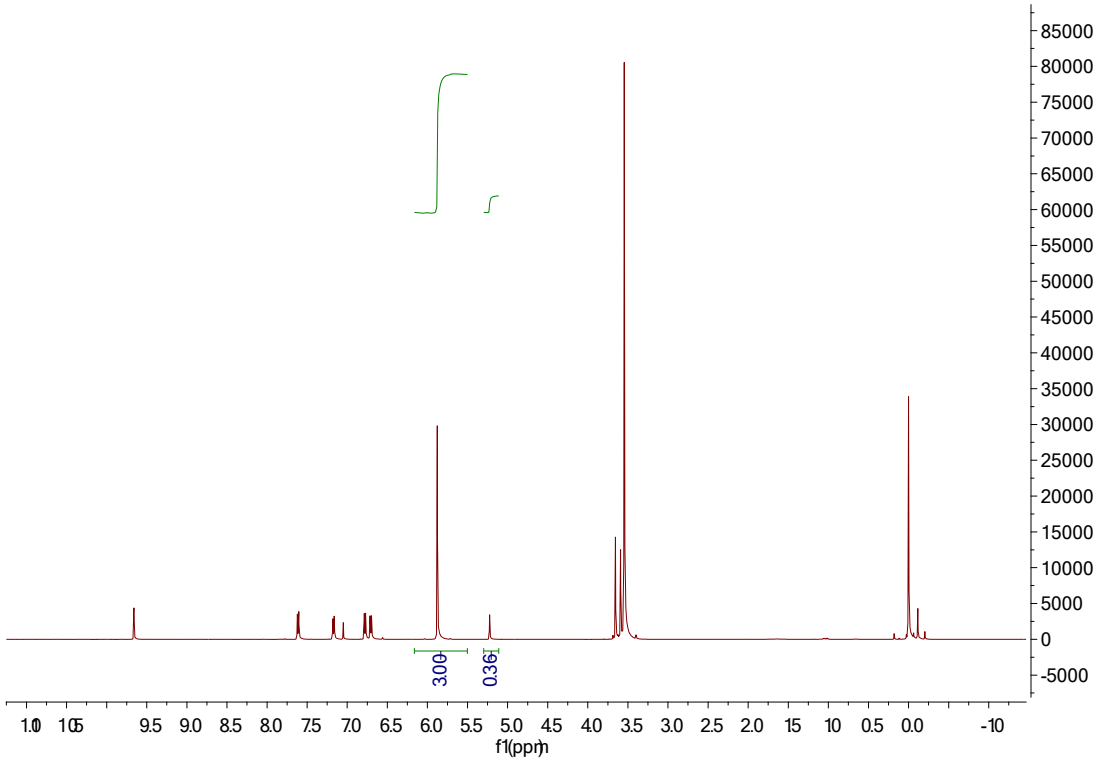

Fig. S29 ^{1}H-NMR for catalysis of 4-methoxybenzaldehyde in DCM with 2.4 eqv TMSCN for 3h.
Yiled = 36%

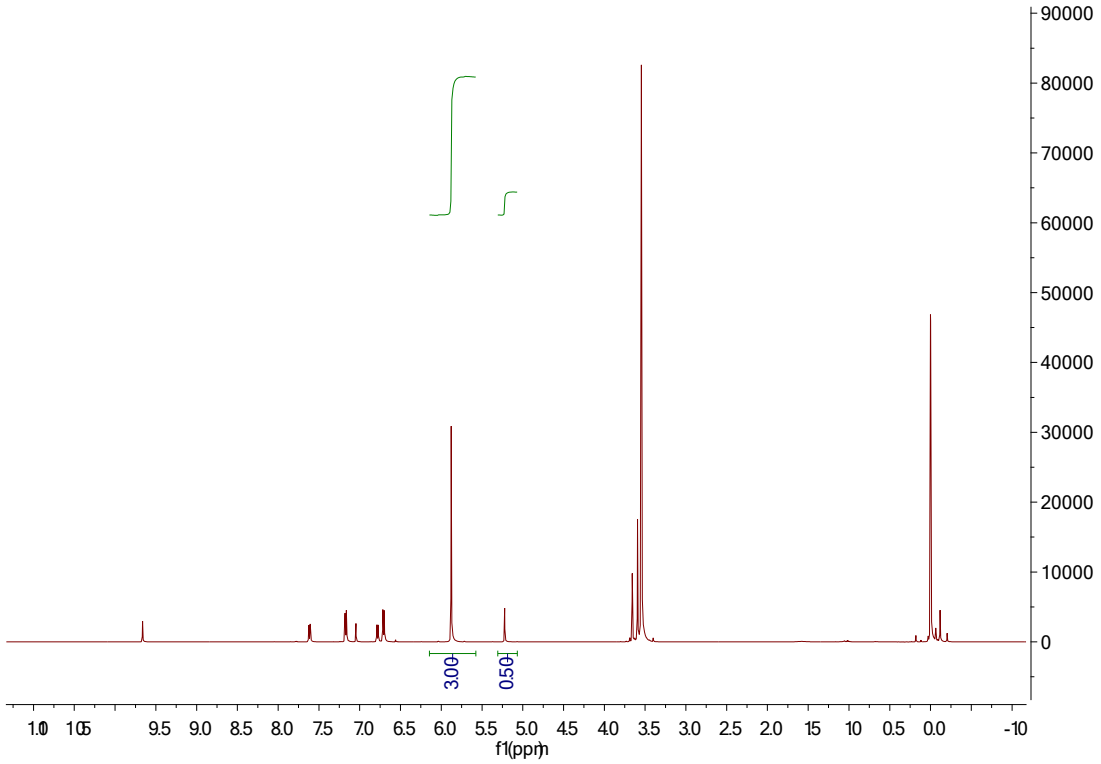

Fig. S30 ^{1}H-NMR for catalysis of 4-methoxybenzaldehyde in DCM with 2.4 eqv TMSCN for 4h.
Yiled = 50%

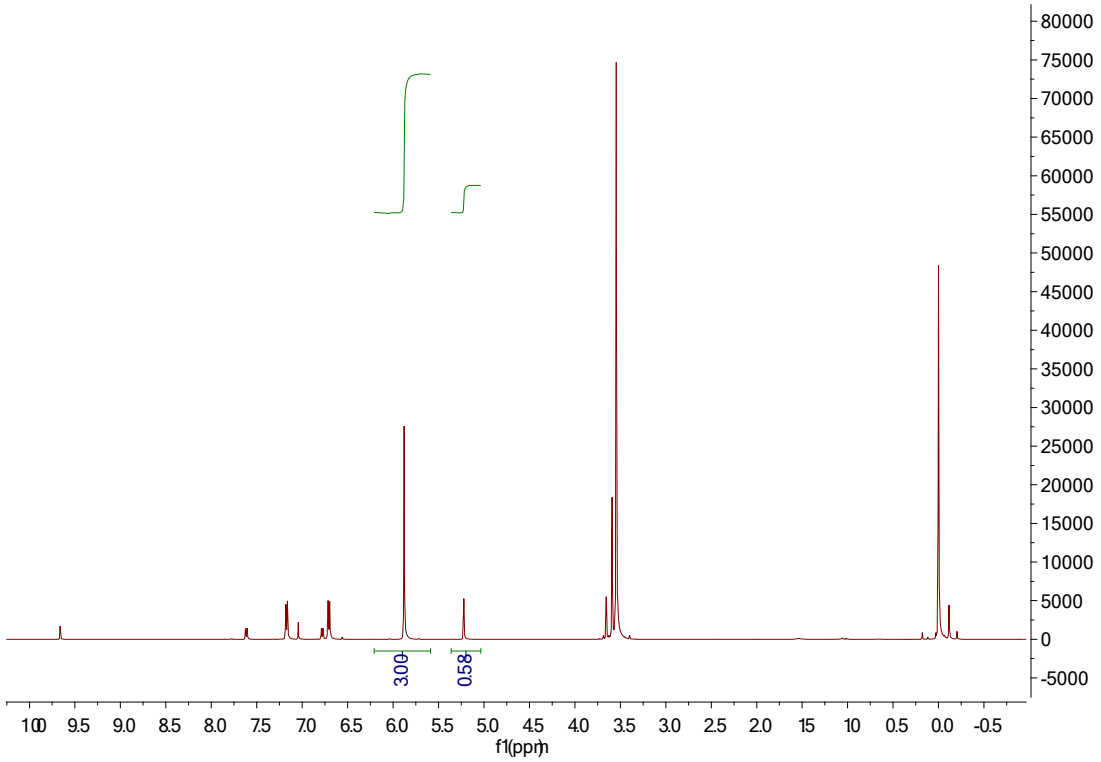

Fig. S31 ^{1}H-NMR for catalysis of 4-methoxybenzaldehyde in DCM with 2.4 eqv TMSCN for 5h.
Yiled = 58%

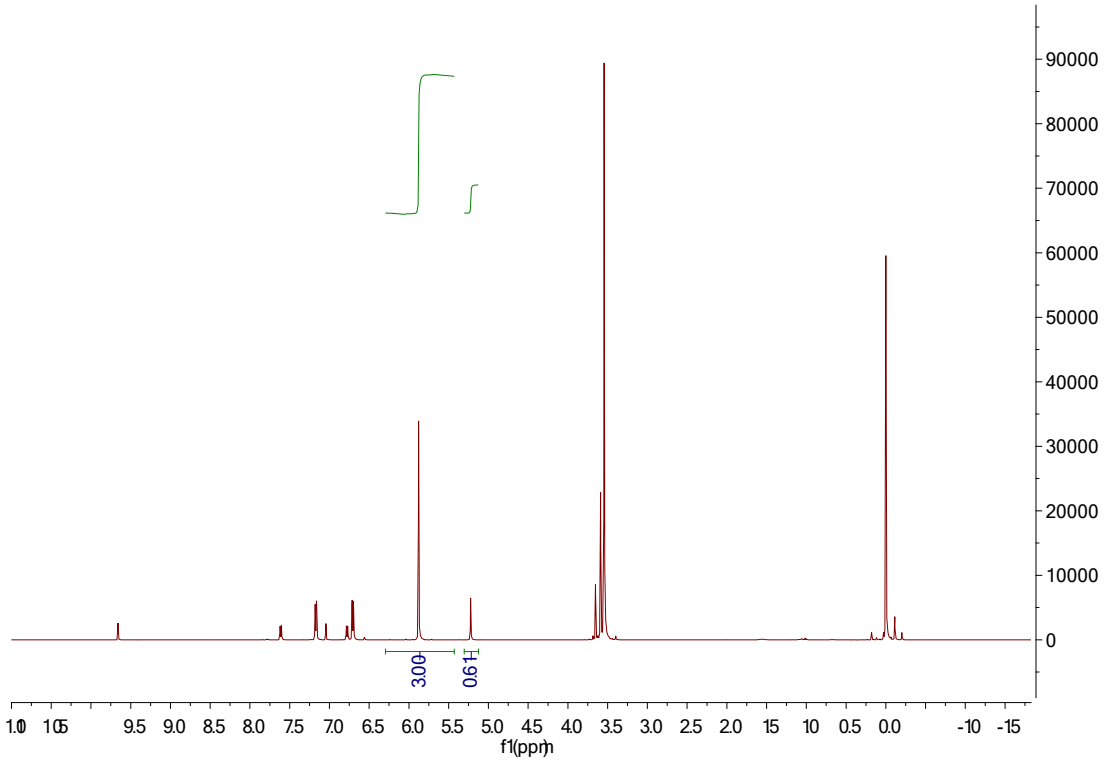

Fig. S32 ^{1}H-NMR for catalysis of 4-methoxybenzaldehyde in DCM with 2.4 eqv TMSCN for 6h.
Yiled = 61%

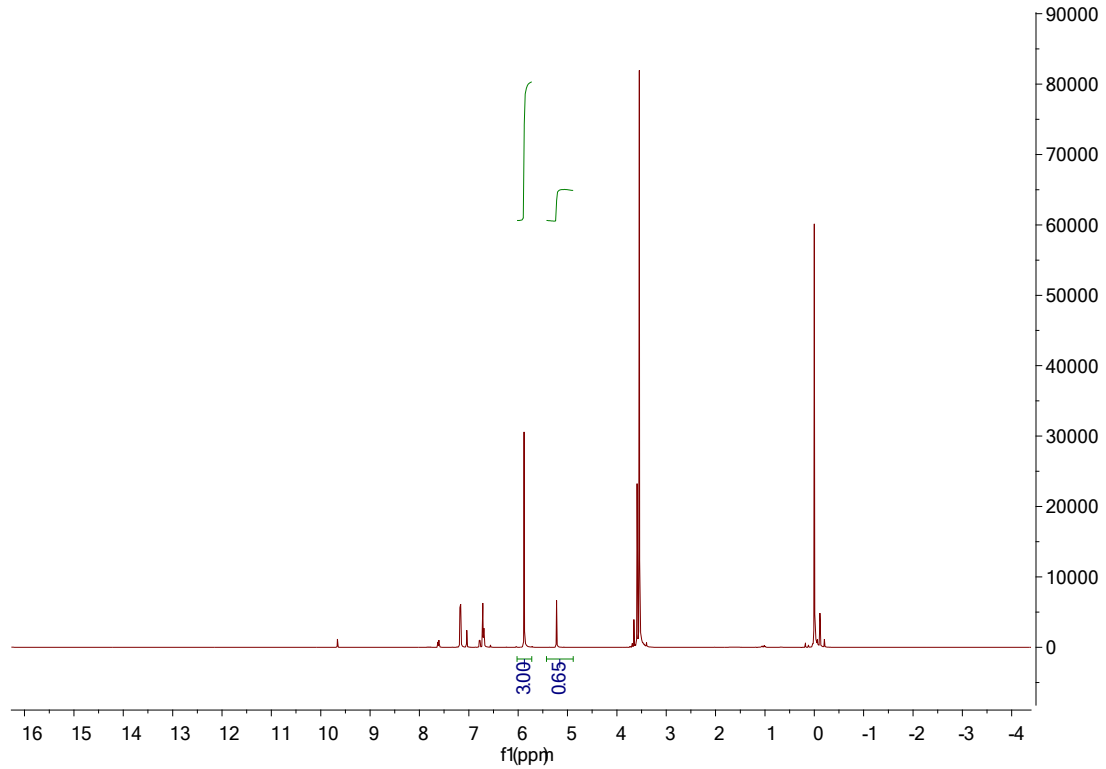

Fig. S33 ^{1}H-NMR for catalysis of 4-methoxybenzaldehyde in DCM with 2.4 eqv TMSCN for 7h.
Yiled = 65%

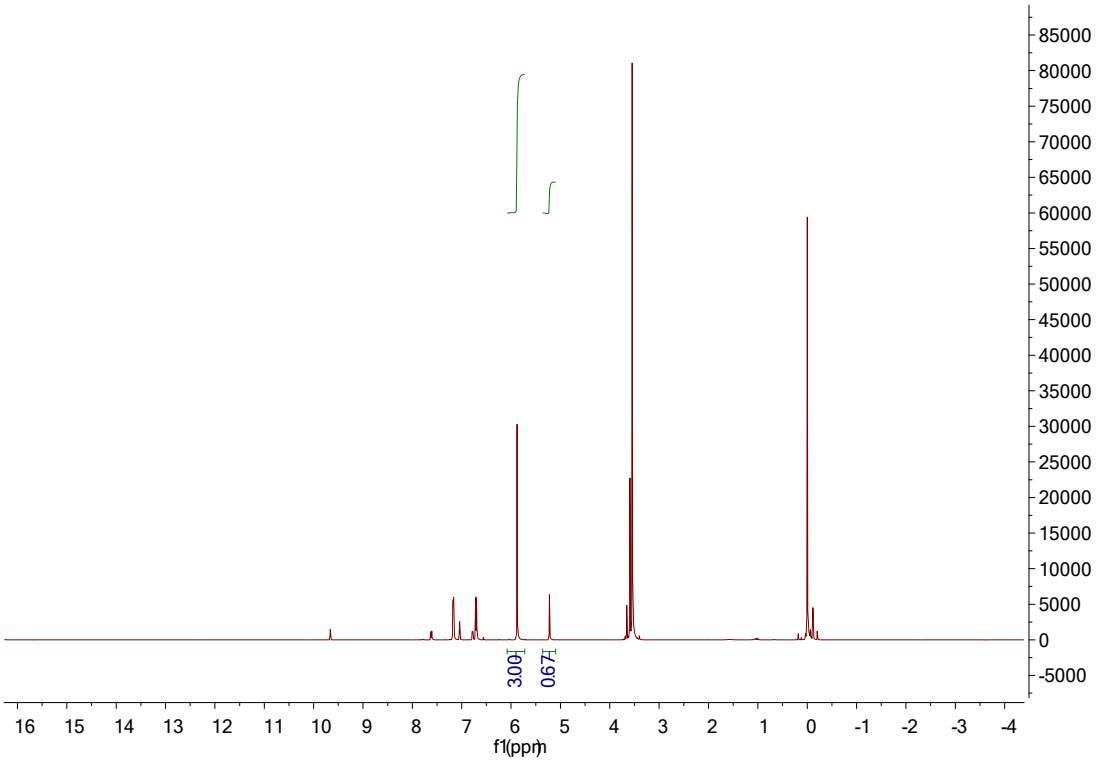

Fig. S34 ^{1}H-NMR for catalysis of 4-methoxybenzaldehyde in DCM with 2.4 eqv TMSCN for 8h.
Yiled = 67%

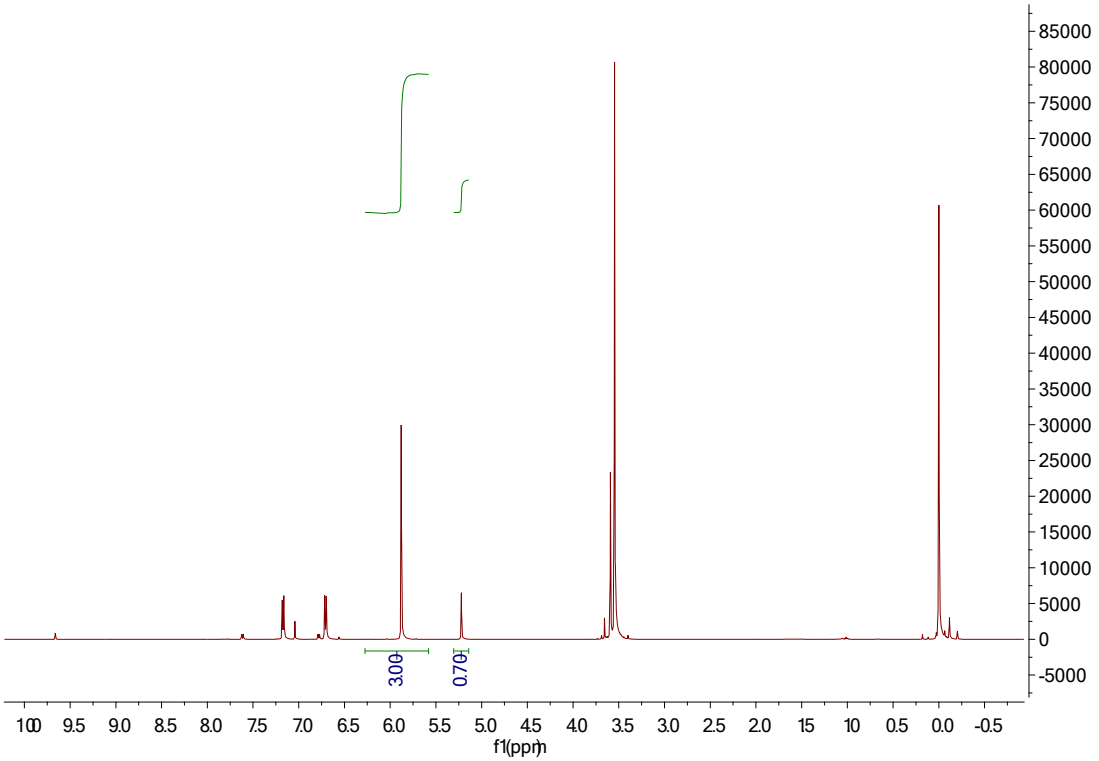

Fig. S35 ^{1}H-NMR for catalysis of 4-methoxybenzaldehyde in DCM with 2.4 eqv TMSCN for 9h.
Yiled = 70%

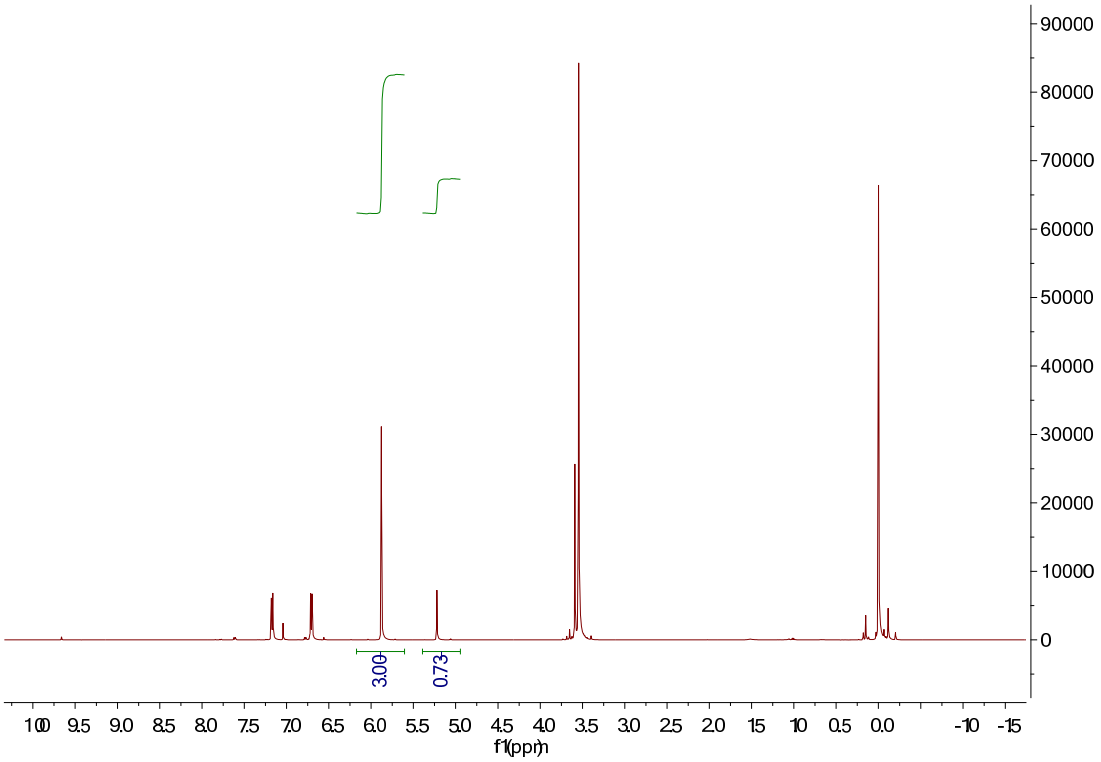

Fig. S36 ^{1}H-NMR for catalysis of 4-methoxybenzaldehyde in DCM with 2.4 eqv TMSCN for 10h.
Yiled = 73%

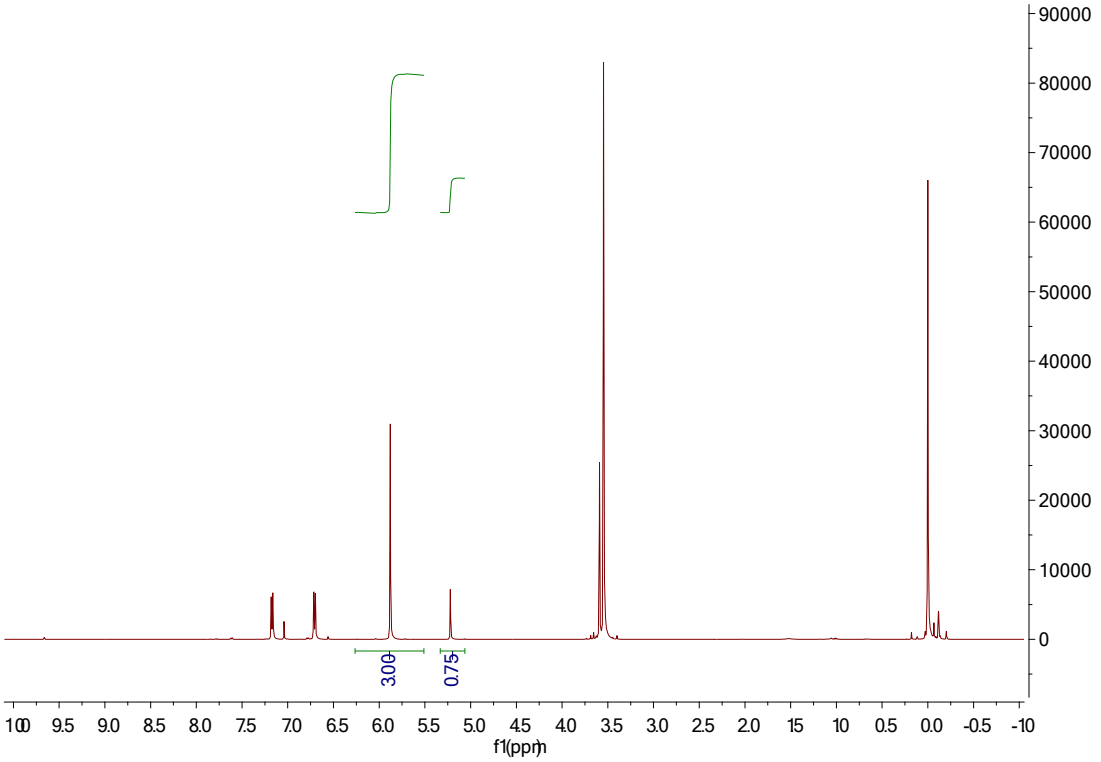

Fig. S37 ^{1}H-NMR for catalysis of 4-methoxybenzaldehyde in DCM with 2.4 eqv TMSCN for 11h.
Yiled = 75%

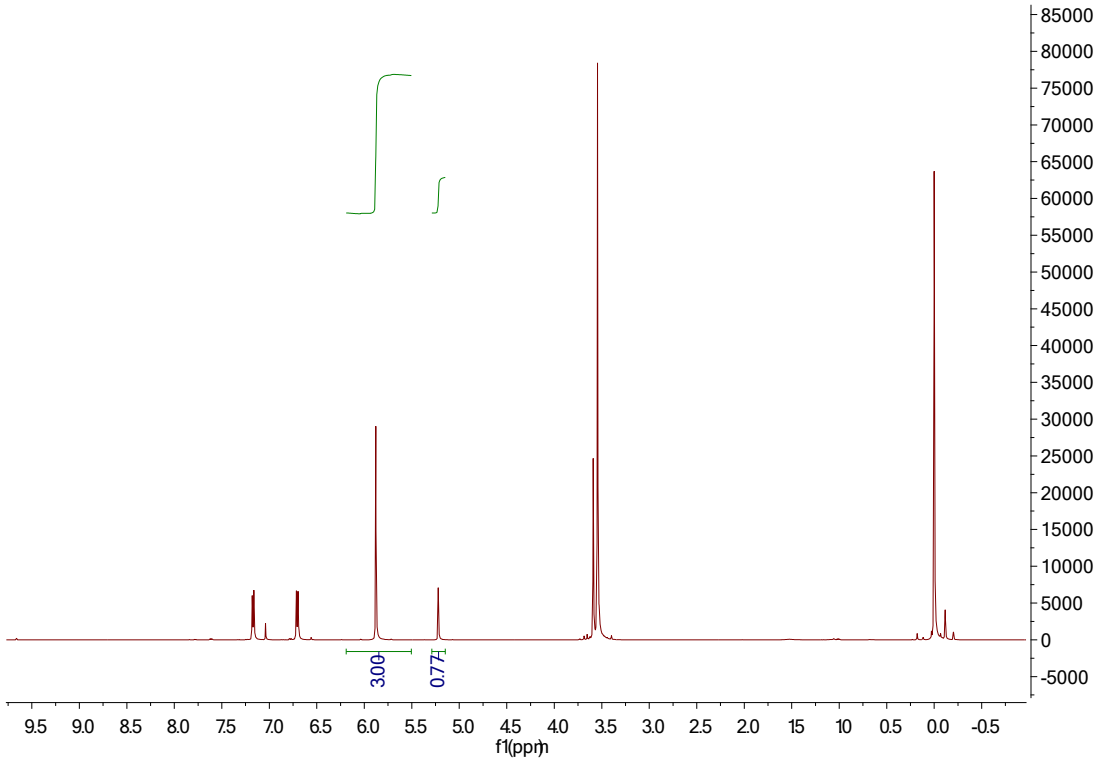

Fig. S38 ^{1}H-NMR for catalysis of 4-methoxybenzaldehyde in DCM with 2.4 eqv TMSCN for 12h.
Yiled = 77%

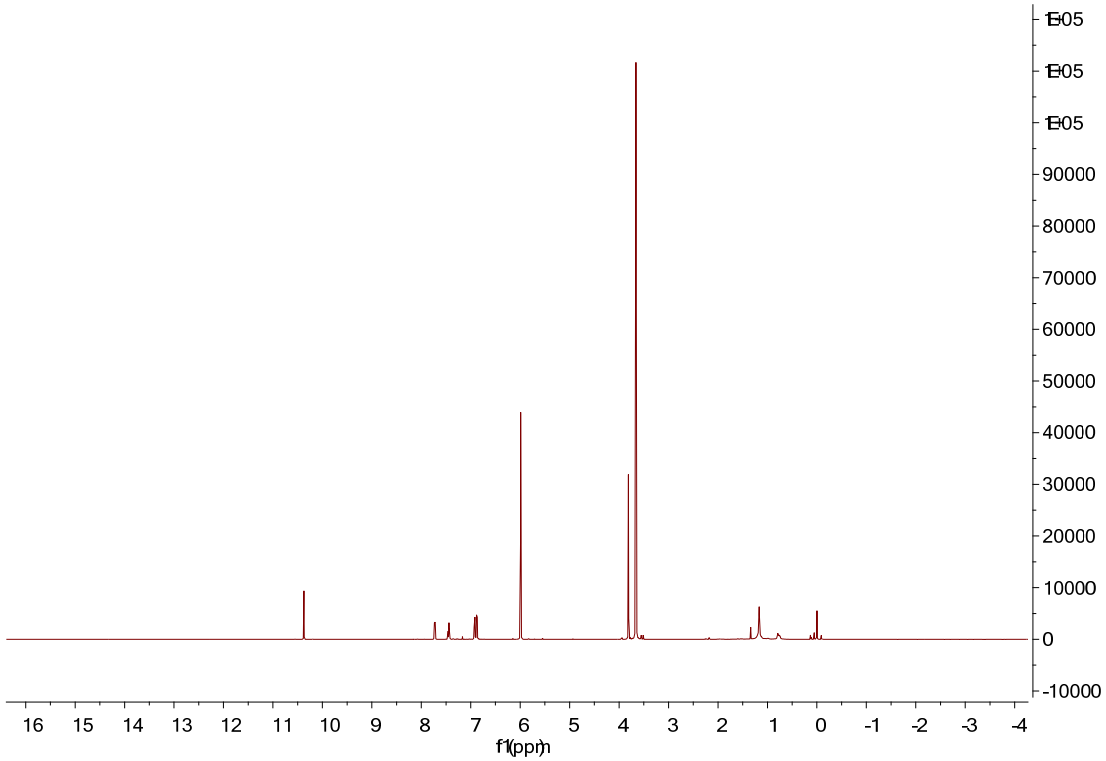

Fig. S39 ^{1}H-NMR for catalysis of 2-methoxybenzaldehyde without any catalyst in DCM with 2.4 eqv TMSCN for 12h.
Yiled = 0%

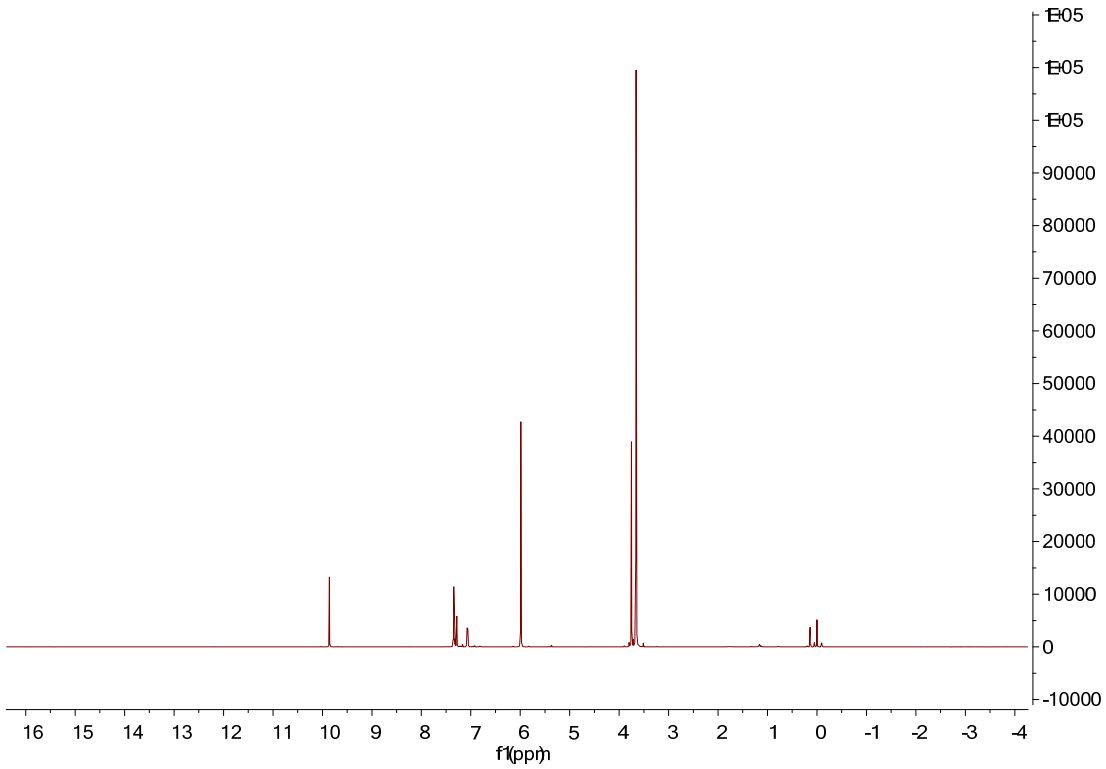

Fig. S40 ^{1}H-NMR for catalysis of 3-methoxybenzaldehyde without any catalyst in DCM with 2.4 eqv TMSCN for 12h.
Yiled = 0%

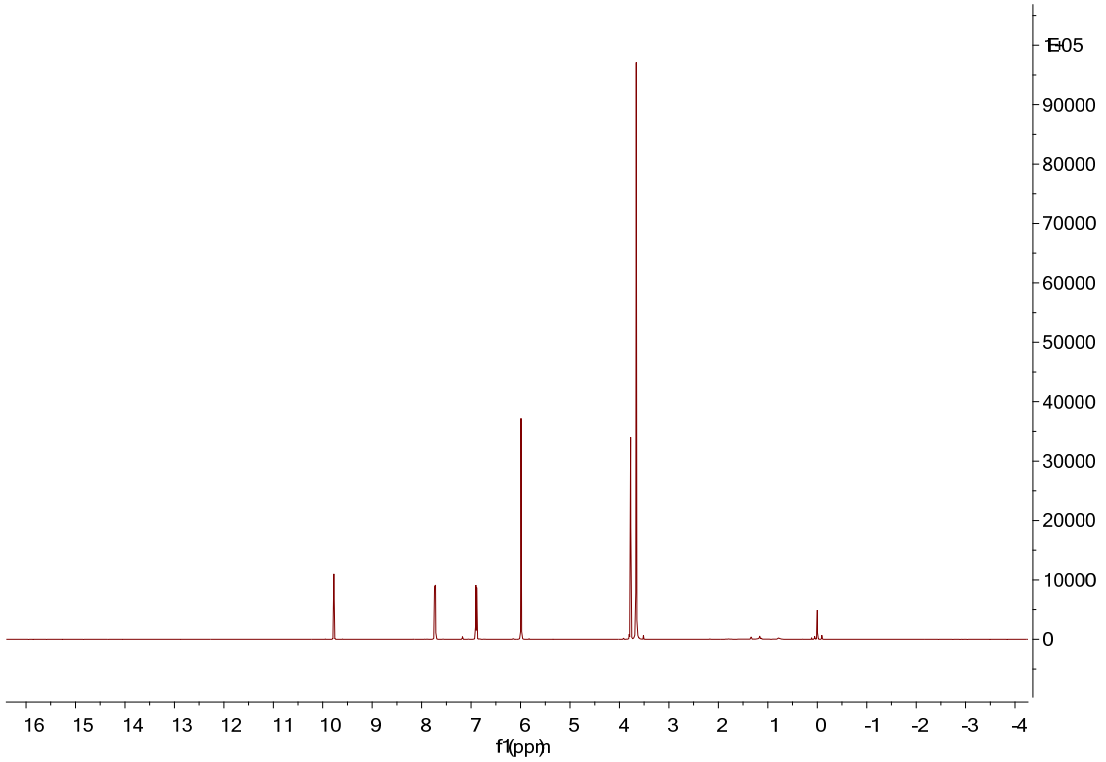

Fig. S41 ^{1}H-NMR for catalysis of 4-methoxybenzaldehyde without any catalyst in DCM with 2.4 eqv TMSCN for 12h.
Yiled = 0%

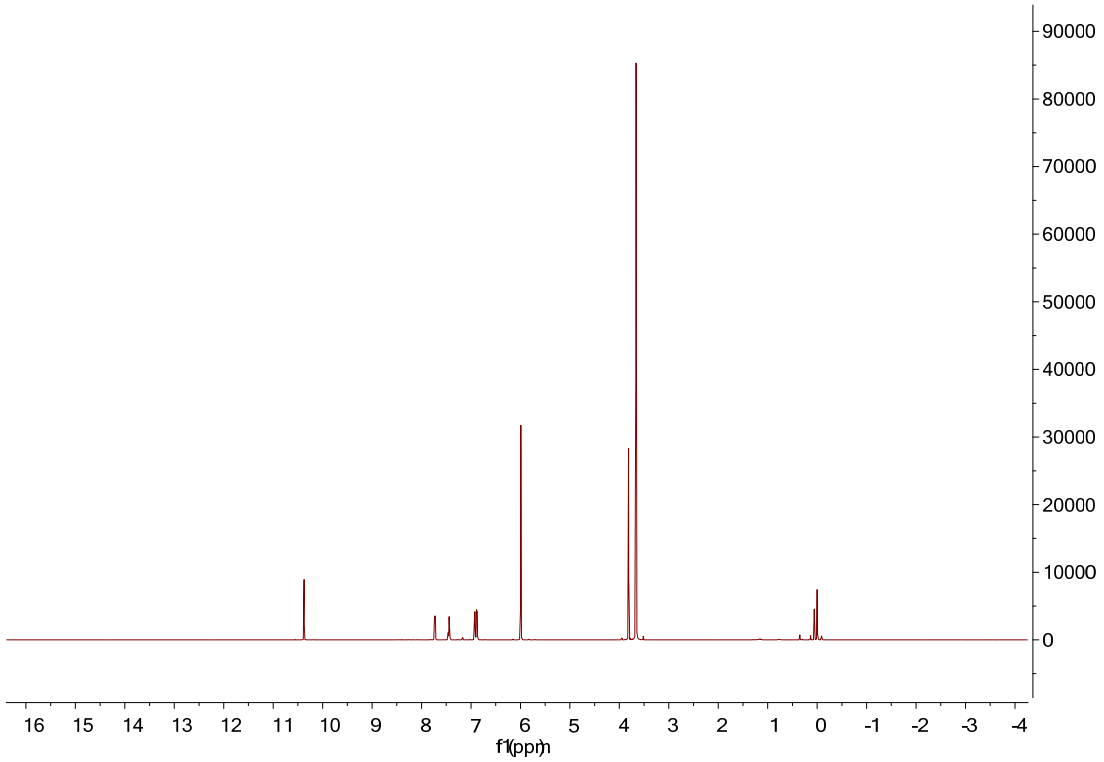

Fig. S42 ^{1}H-NMR for catalysis of 2-methoxybenzaldehyde with H_2sbdc as the catalyst in DCM with 2.4 eqv TMSCN for 12h.
Yiled = 0%

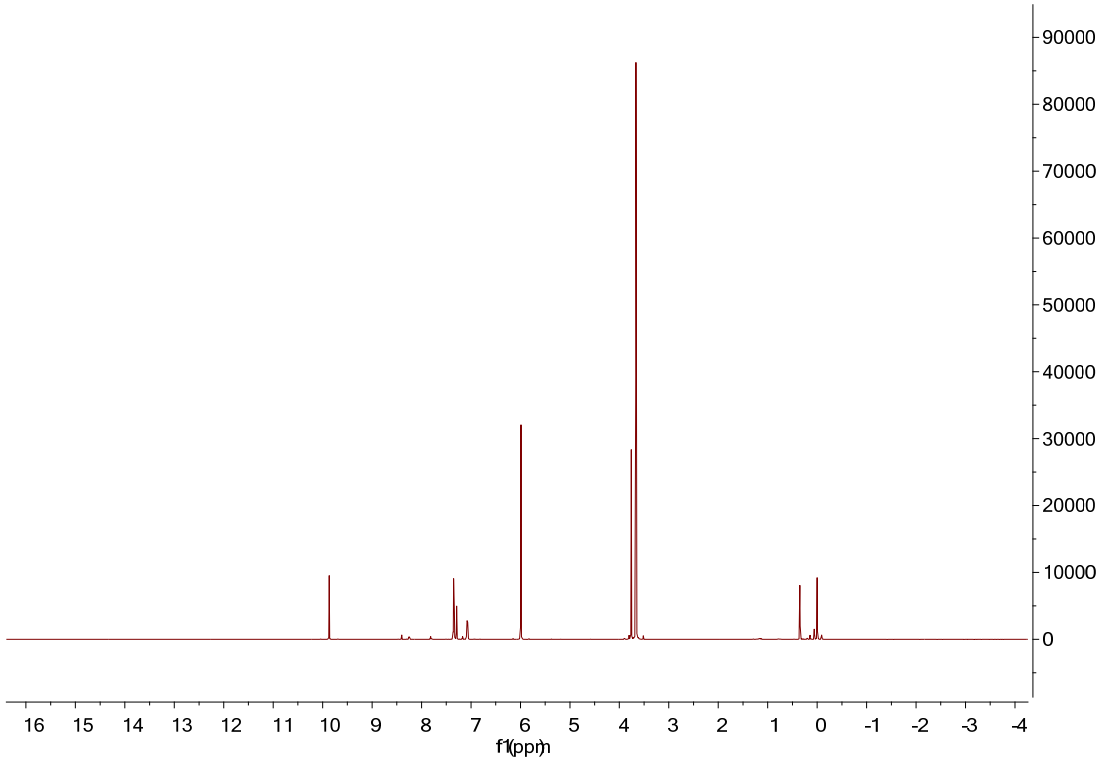

Fig. S43 ^{1}H-NMR for catalysis of 3-methoxybenzaldehyde with H_2sbdc as the catalyst in DCM with 2.4 eqv TMSCN for 12h.
Yiled = 0%

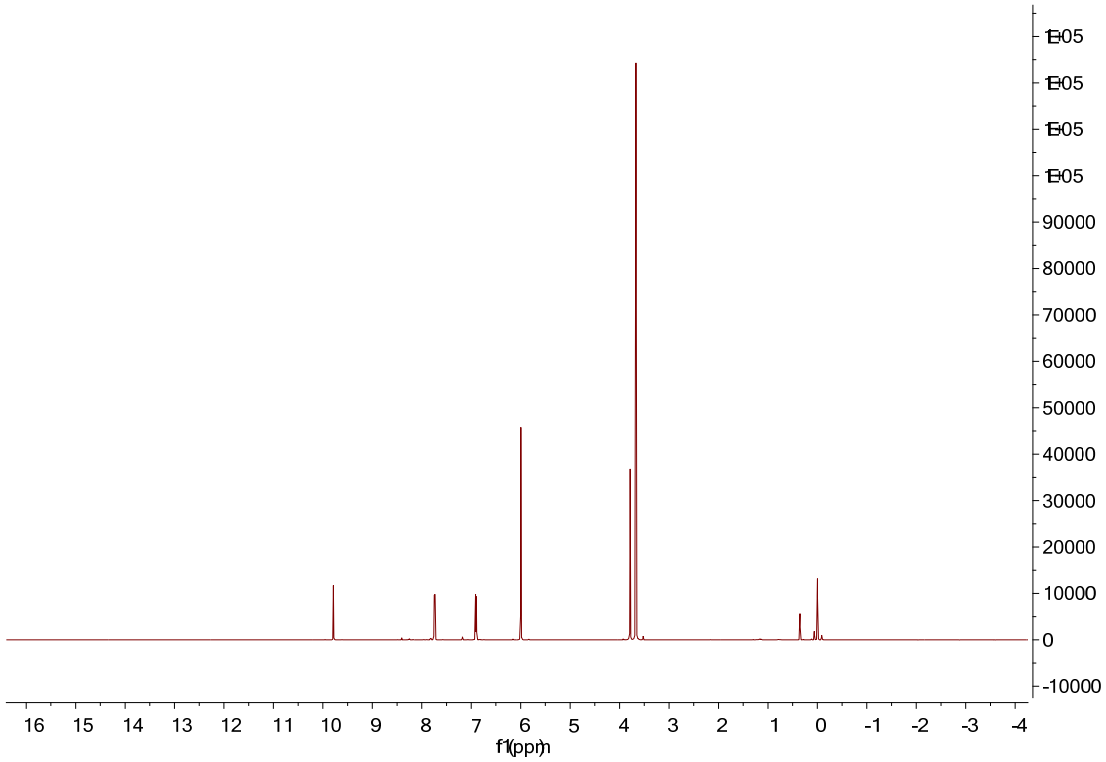

Fig. S44 ^{1}H-NMR for catalysis of 4-methoxybenzaldehyde with H_2sbdc as the catalyst in DCM with 2.4 eqv TMSCN for 12h.
Yiled = 0%

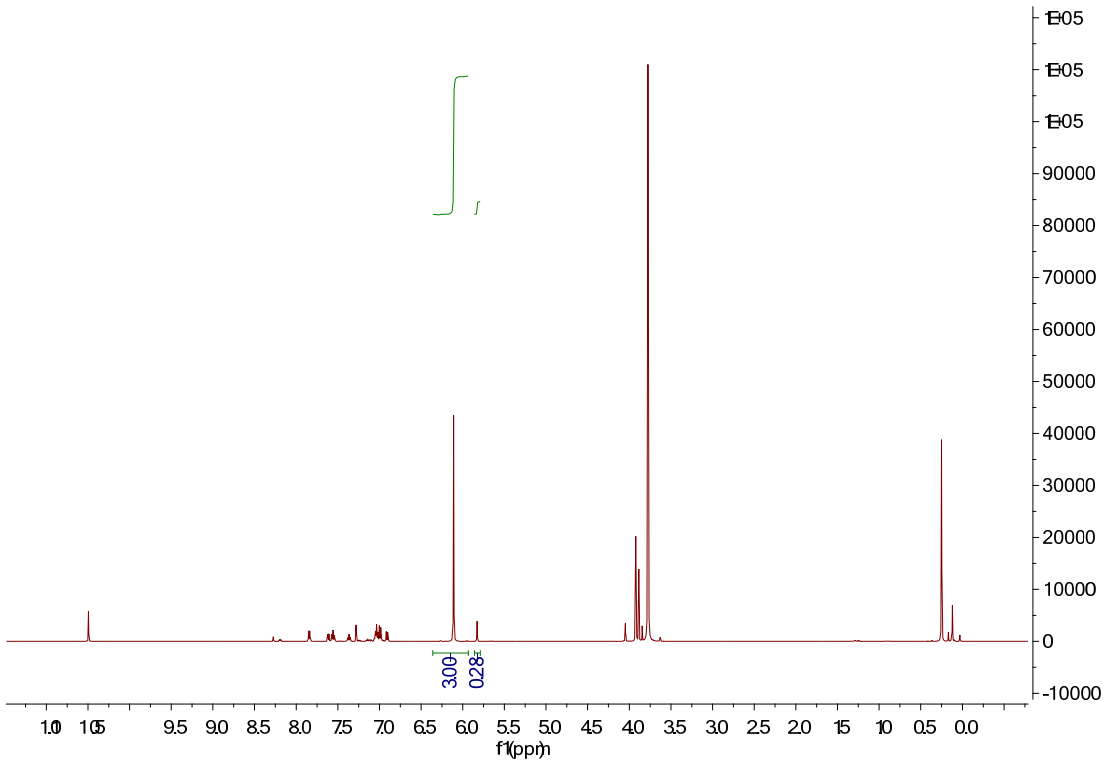

Fig. S45 ^{1}H-NMR for catalysis of 2-methoxybenzaldehyde in DCM with 2.4 eqv TMSCN for 4h.
Yiled = 28%

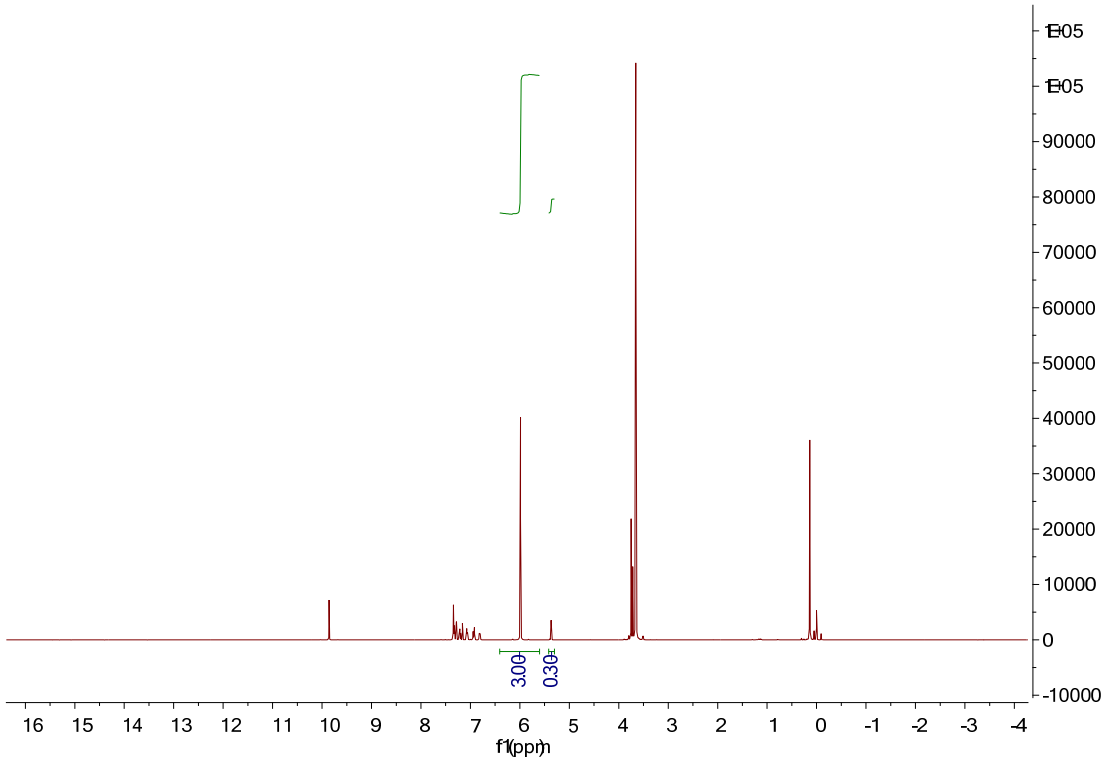

Fig. S46 ^{1}H-NMR for catalysis of 3-methoxybenzaldehyde in DCM with 2.4 eqv TMSCN for 4h.
Yiled = 30%

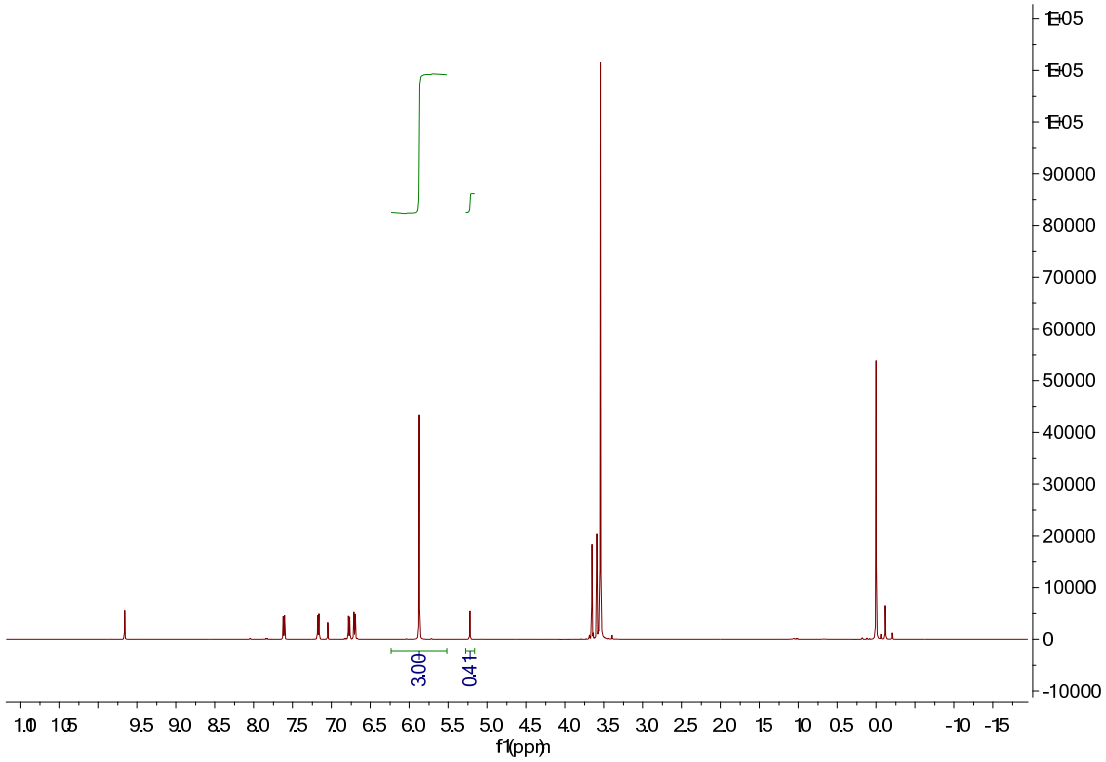

Fig. S47 ^{1}H-NMR for catalysis of 4-methoxybenzaldehyde in DCM with 2.4 eqv TMSCN for 4h.
Yiled = 41%

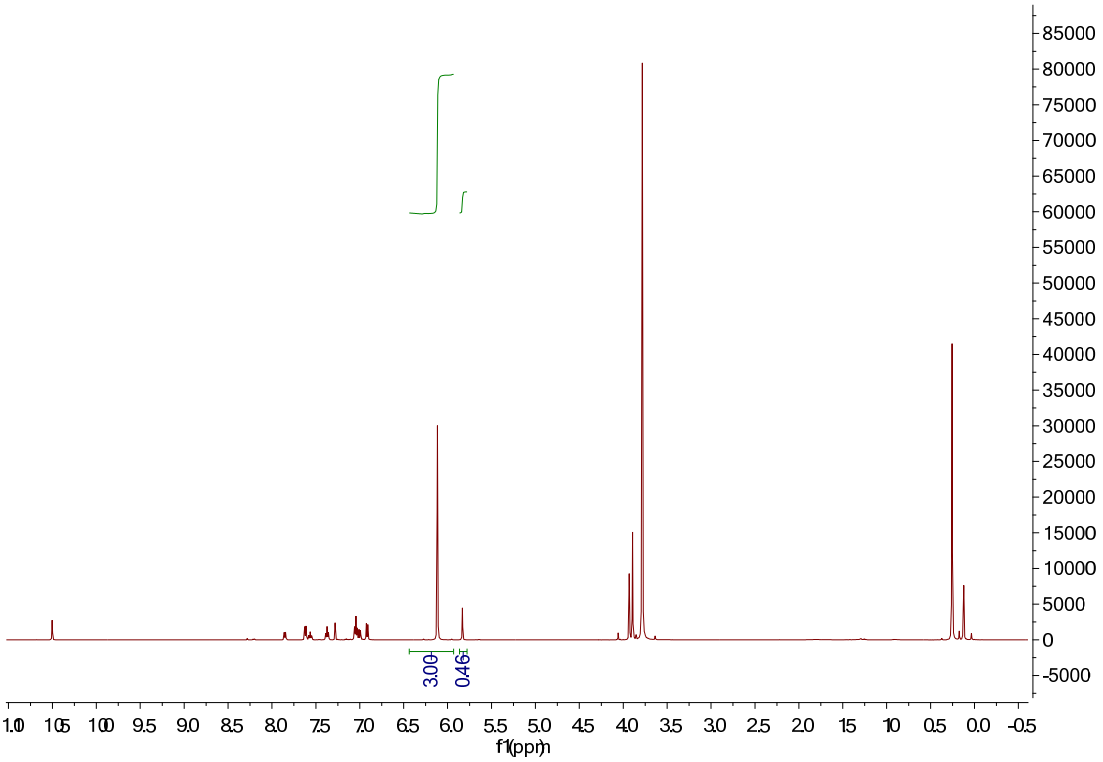

Fig. S48 ^{1}H-NMR for catalysis of 2-methoxybenzaldehyde in DCM with 2.4 eqv TMSCN for 12h (catalyst filtered at 4h).
Yiled = 46%

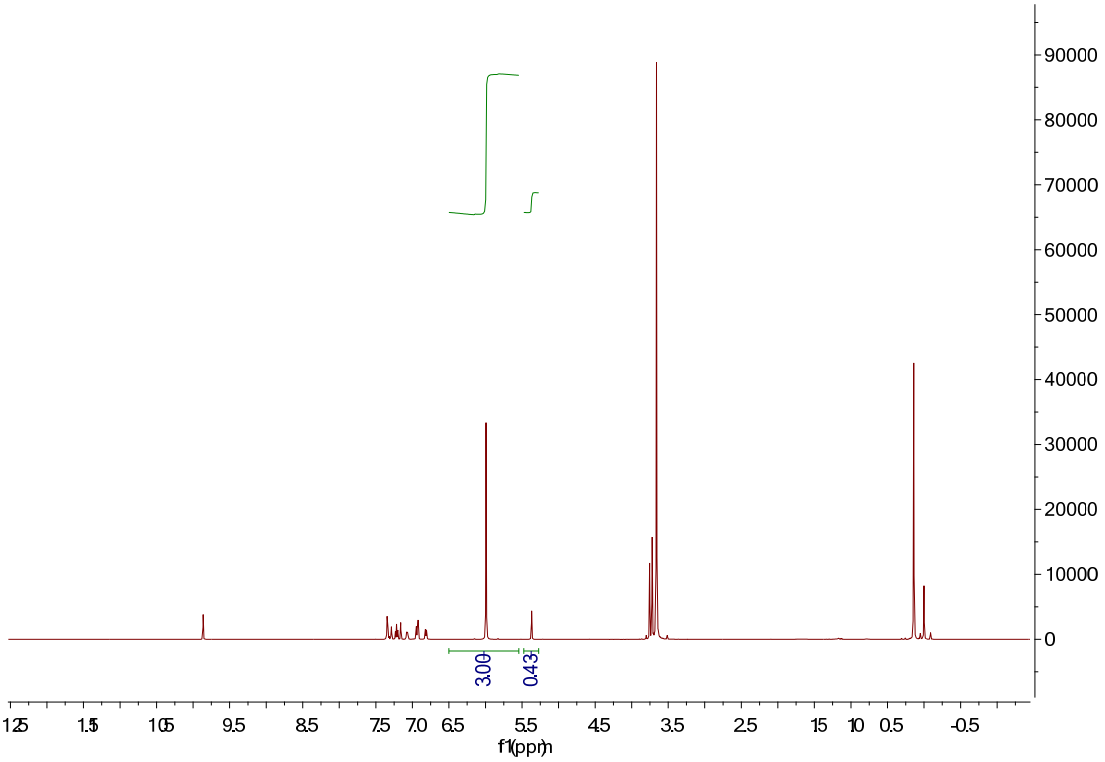

Fig. S49 ^{1}H-NMR for catalysis of 3-methoxybenzaldehyde in DCM with 2.4 eqv TMSCN for 12h (catalyst filtered at 4h).
Yiled = 43%

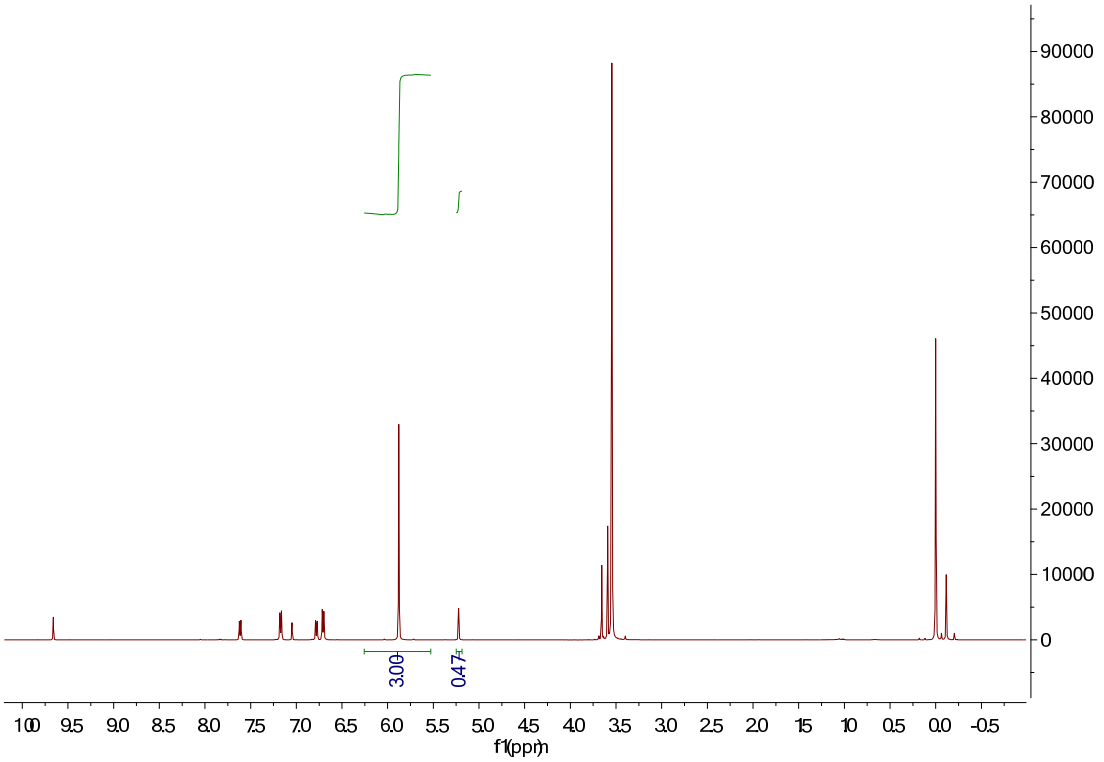

Fig. S50 ^{1}H-NMR for catalysis of 4-methoxybenzaldehyde in DCM with 2.4 eqv TMSCN for 12h (catalyst filtered at 4h).
Yiled = 47%

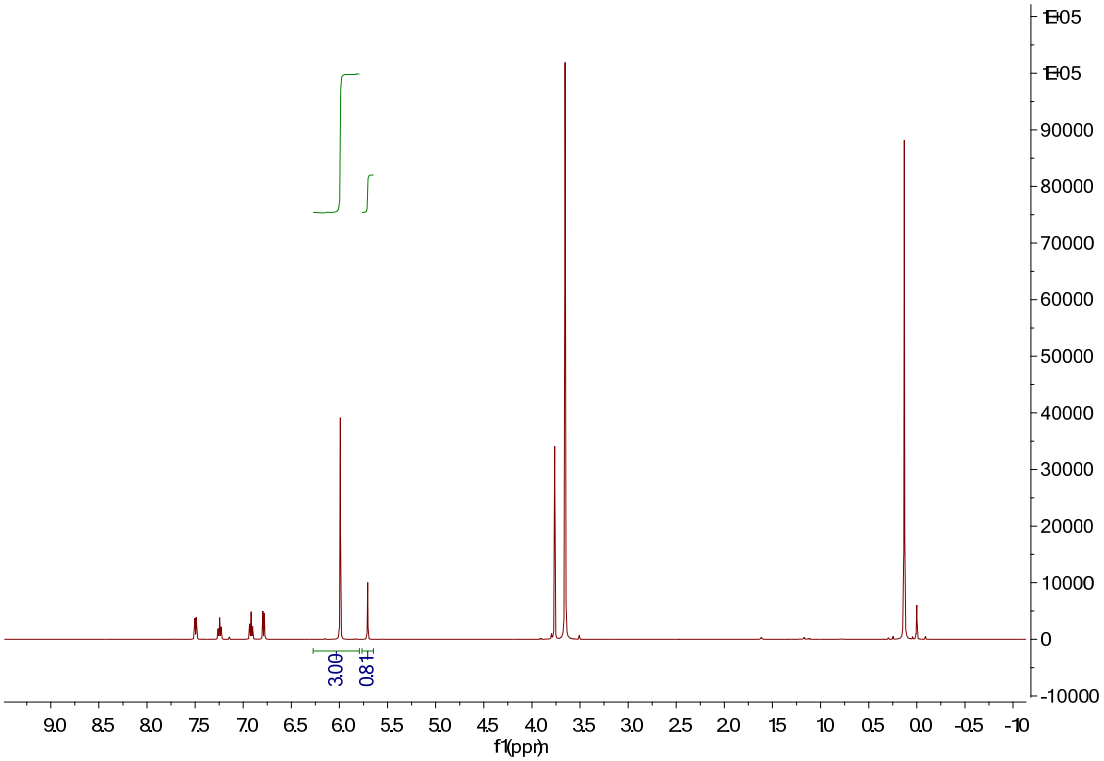

Fig. S51 ^{1}H-NMR for catalysis of 2-methoxybenzaldehyde with 2 eqv catalyst in DCM with 2.4 eqv TMSCN for 12h.
Yiled = 81%

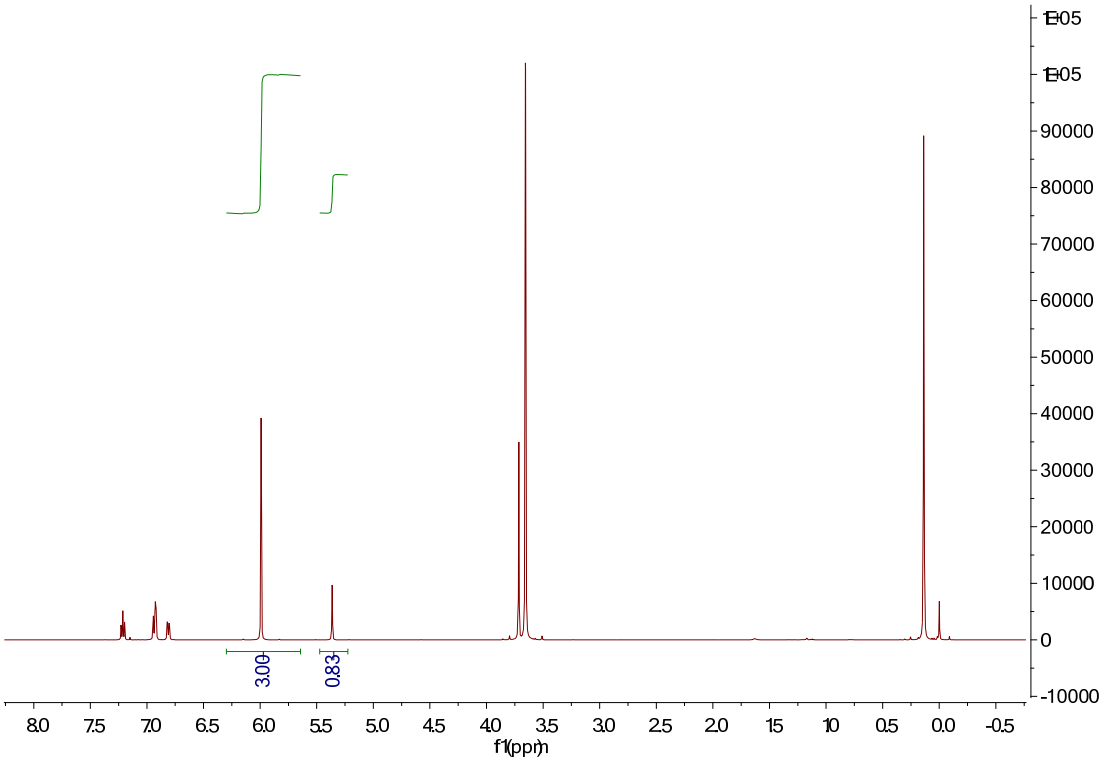

Fig. S52 ^{1}H-NMR for catalysis of 3-methoxybenzaldehyde with 2 eqv catalyst in DCM with 2.4 eqv TMSCN for 12h.
Yiled = 83%

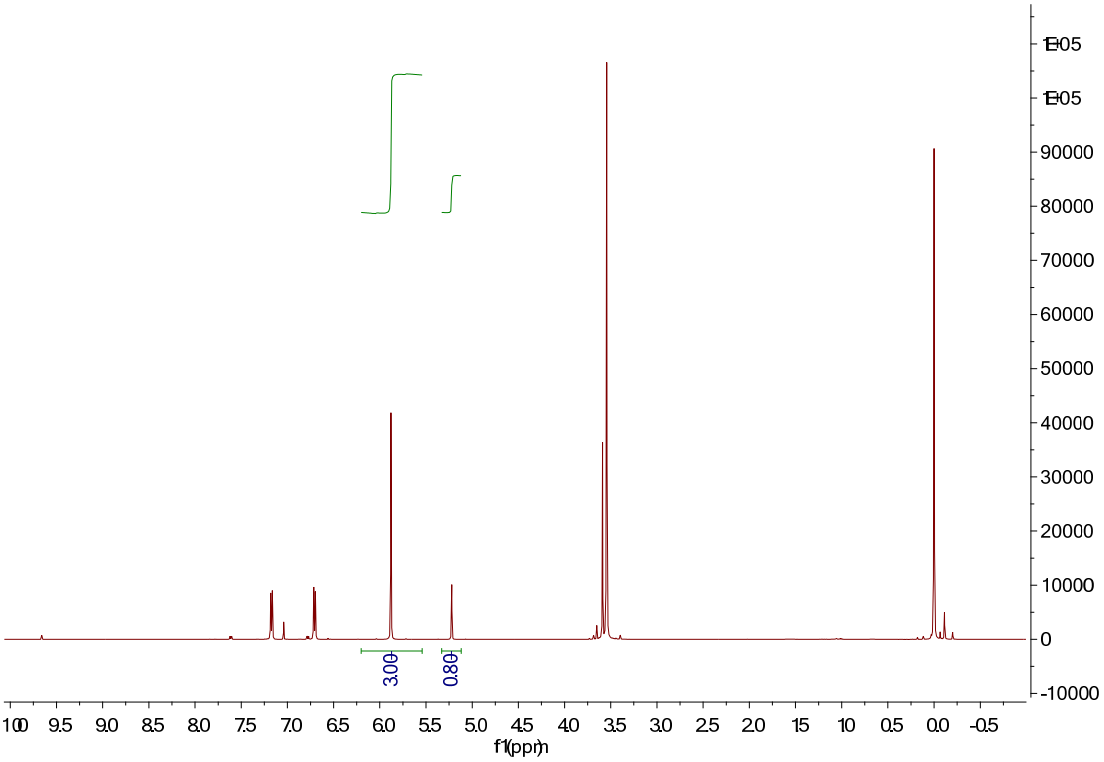

Fig. S53 ^{1}H-NMR for catalysis of 4-methoxybenzaldehyde with 2 eqv catalyst in DCM with 2.4 eqv TMSCN for 12h.
Yiled = 80%

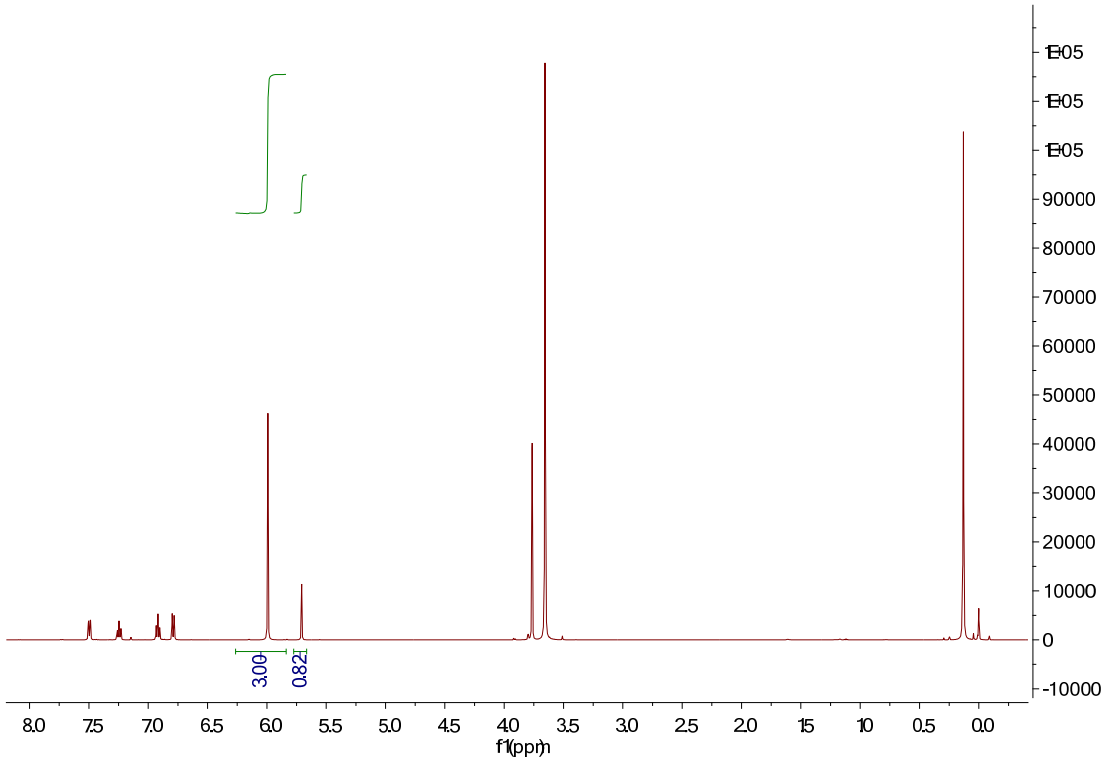

Fig. S54 ^{1}H-NMR for catalysis of 2-methoxybenzaldehyde with in DCM with 2.4 eqv TMSCN for 12h for the second cycle.
Yiled = 82%

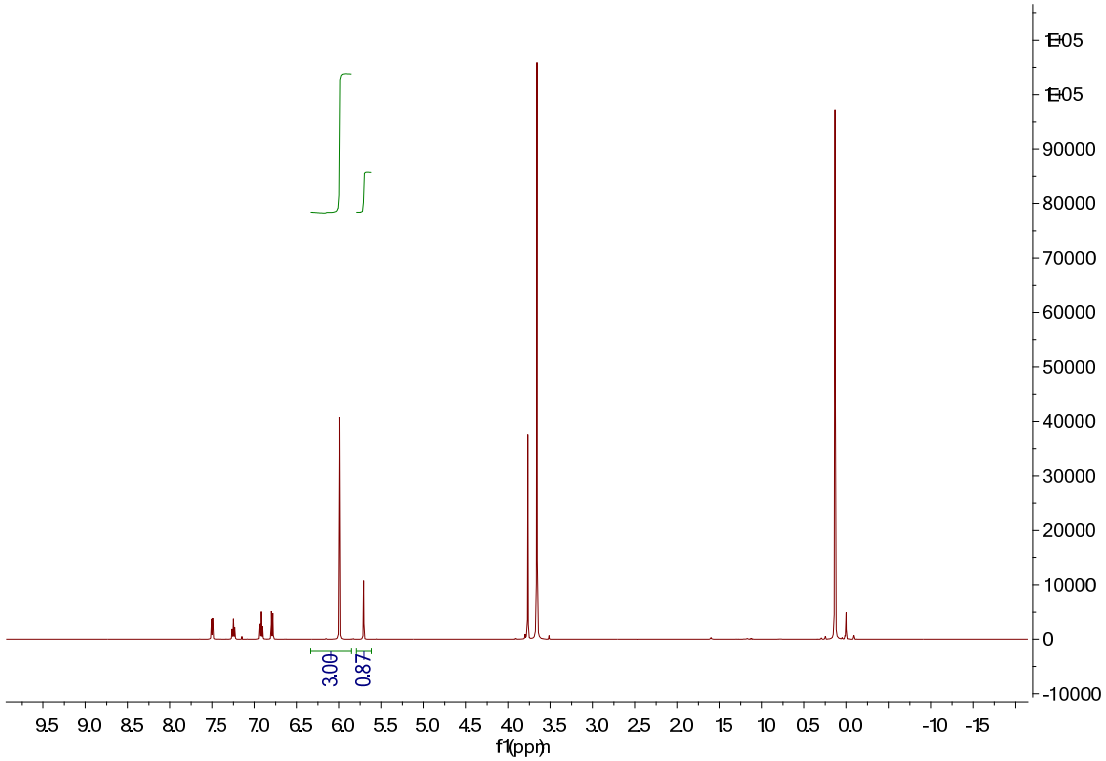

Fig. S55 ^{1}H-NMR for catalysis of 2-methoxybenzaldehyde with in DCM with 2.4 eqv TMSCN for 12h for the third cycle.
Yiled = 87%

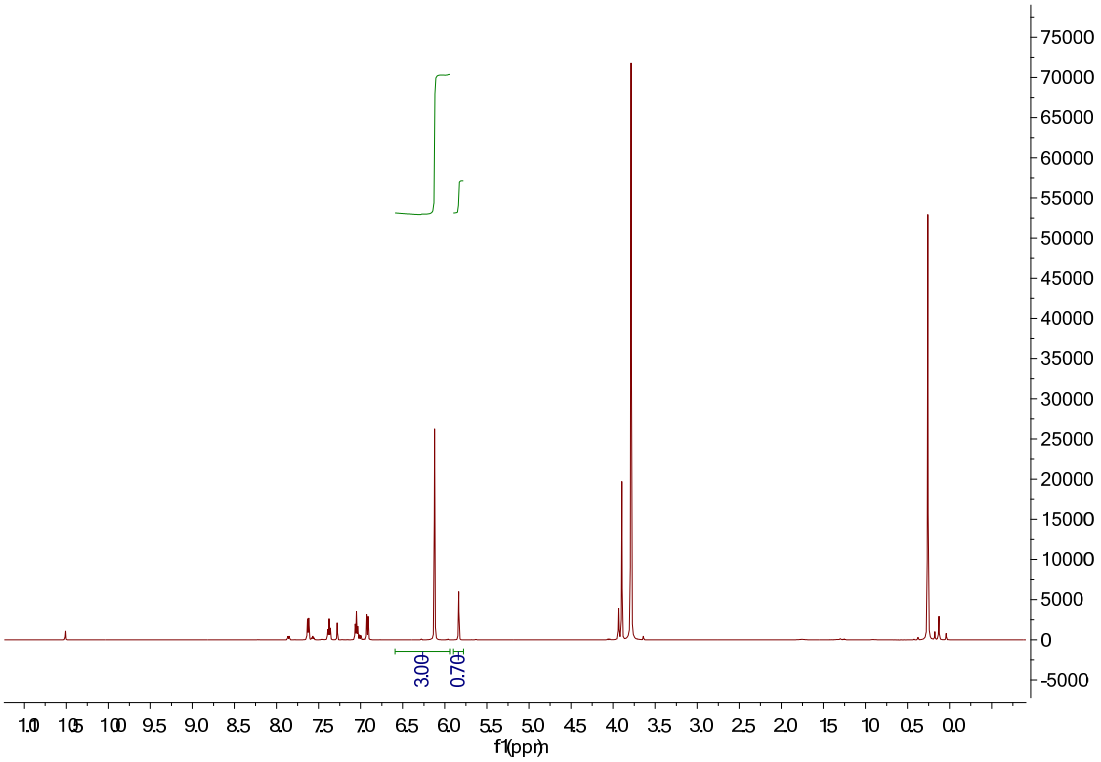

Fig. S56 ^{1}H-NMR for catalysis of 2-methoxybenzaldehyde with in DCM with 2.4 eqv TMSCN for 12h for the forth cycle.
Yiled = 70%

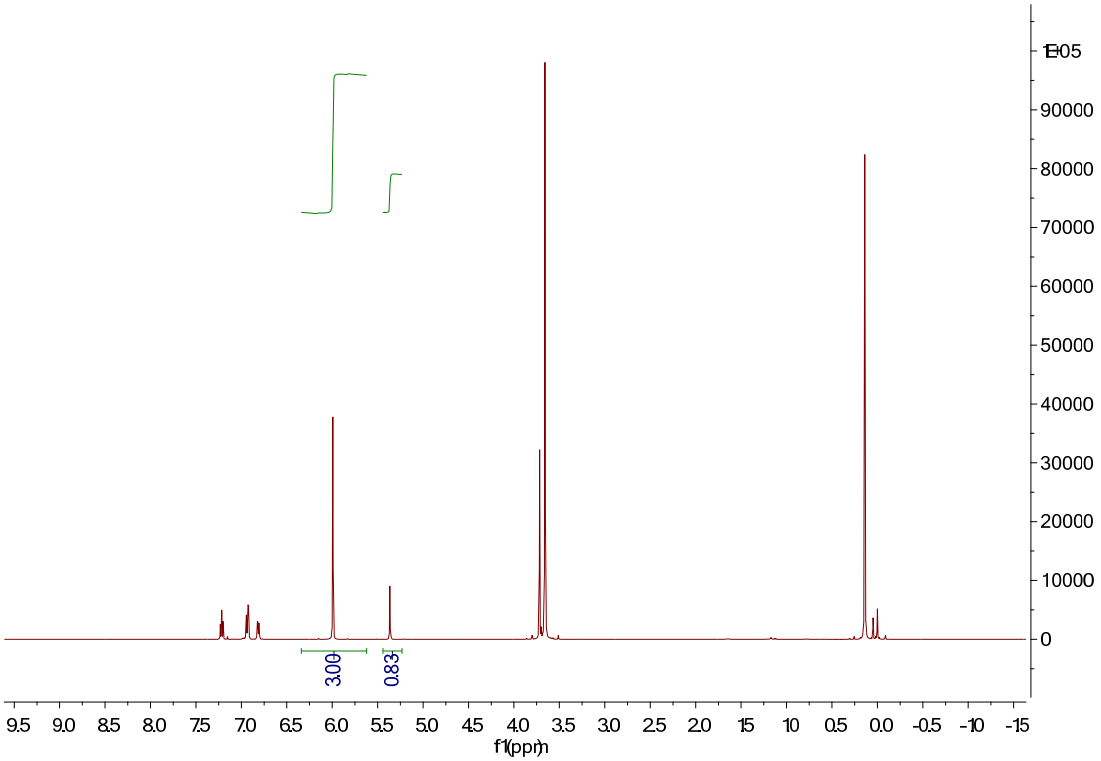

Fig. S57 ^{1}H-NMR for catalysis of 3-methoxybenzaldehyde with in DCM with 2.4 eqv TMSCN for 12h for the second cycle.
Yiled = 83%

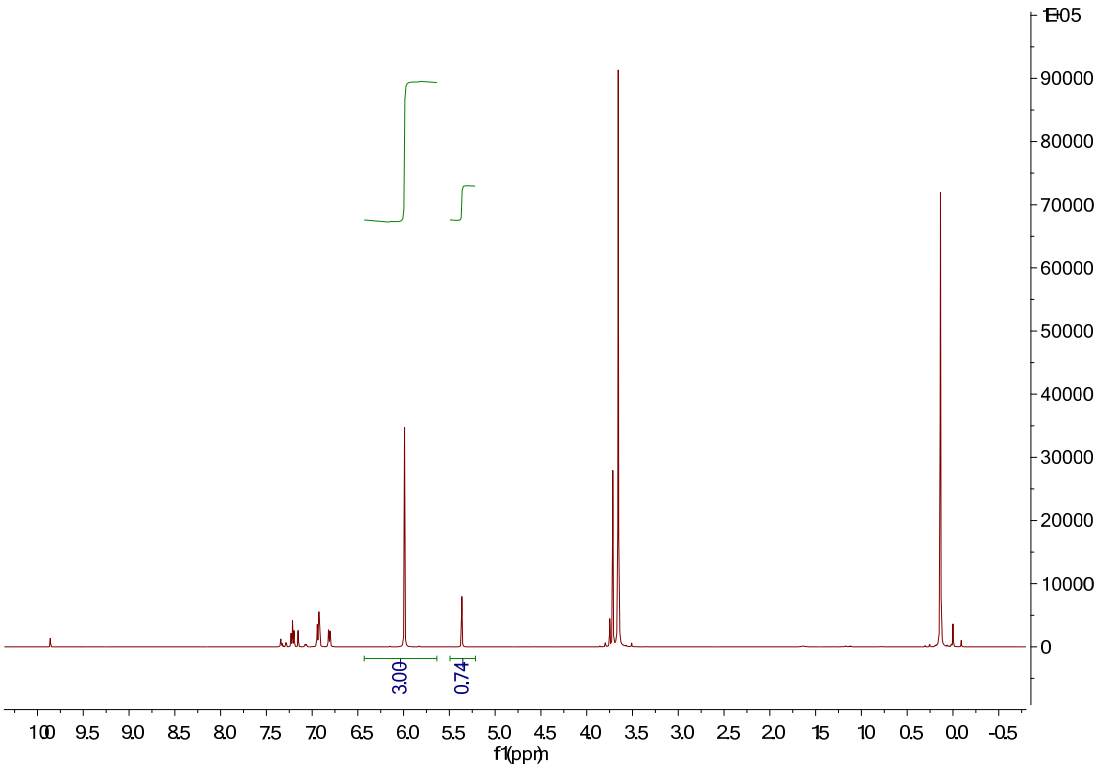

Fig. S58 ^{1}H-NMR for catalysis of 3-methoxybenzaldehyde with in DCM with 2.4 eqv TMSCN for 12h for the third cycle.
Yiled = 74%

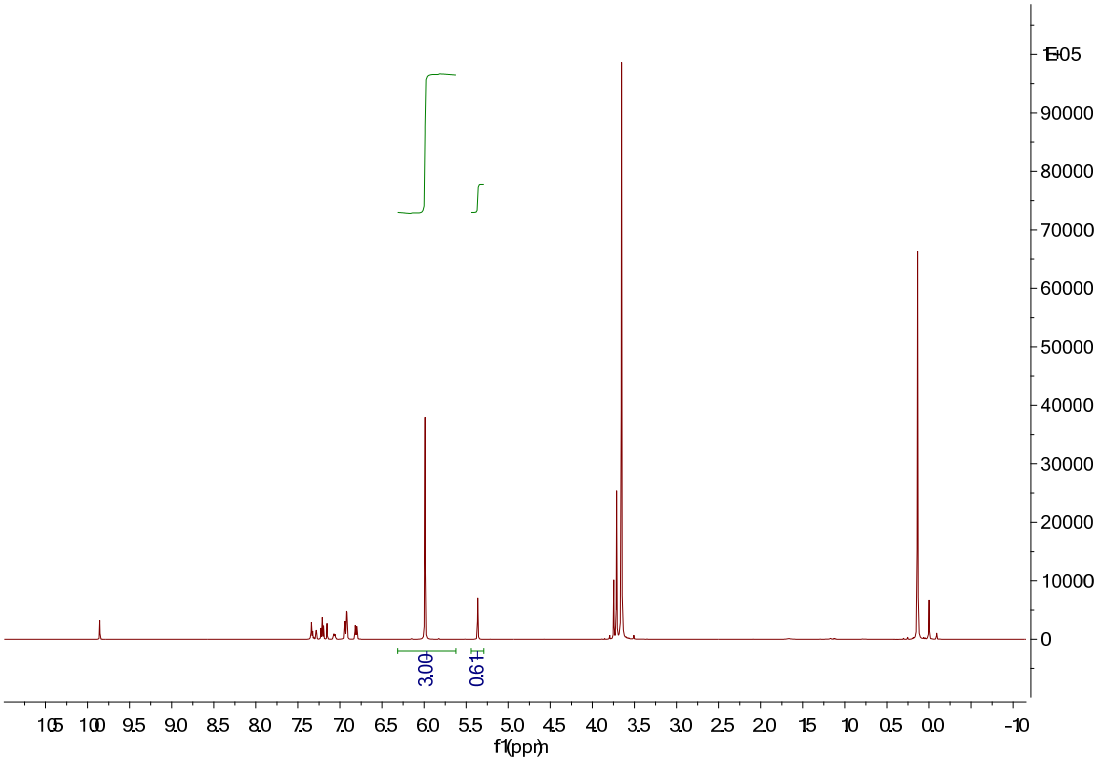

Fig. S59 ^{1}H-NMR for catalysis of 3-methoxybenzaldehyde with in DCM with 2.4 eqv TMSCN for 12h for the forth cycle.
Yiled = 61%

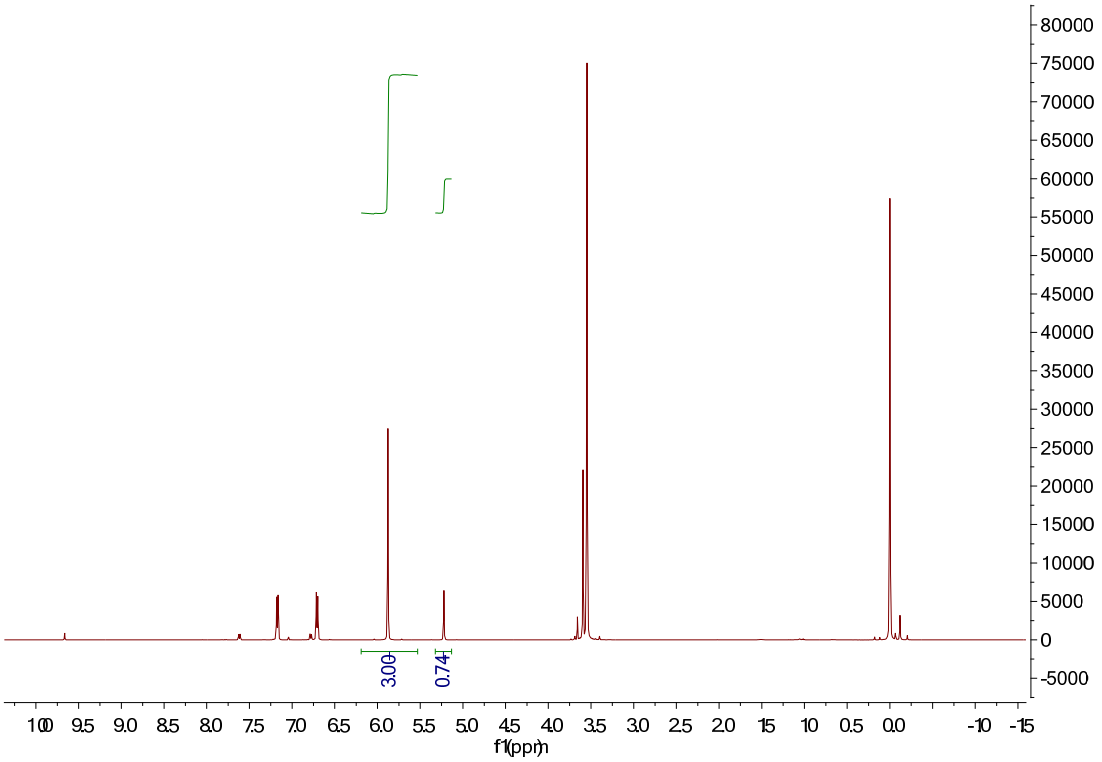

Fig. S60 ^{1}H-NMR for catalysis of 4-methoxybenzaldehyde with in DCM with 2.4 eqv TMSCN for 12h for the forth cycle.
Yiled = 74%

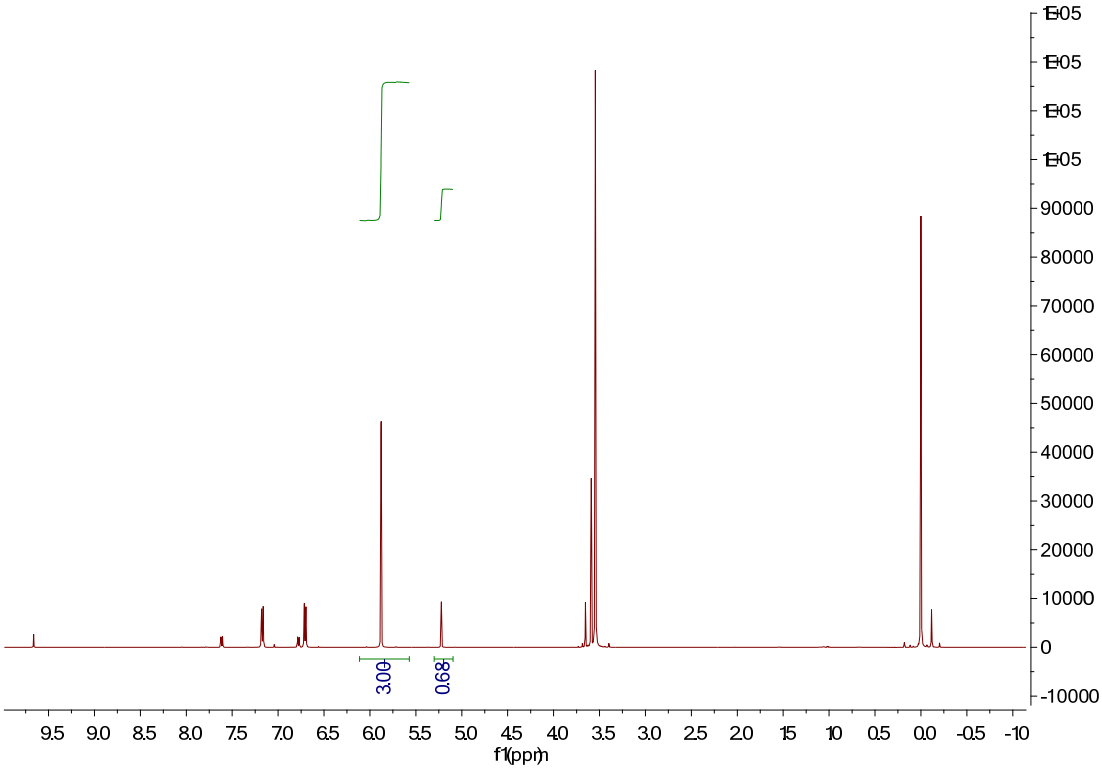

Fig. S61 ^{1}H-NMR for catalysis of 4-methoxybenzaldehyde with in DCM with 2.4 eqv TMSCN for 12h for the forth cycle.
Yiled = 68%

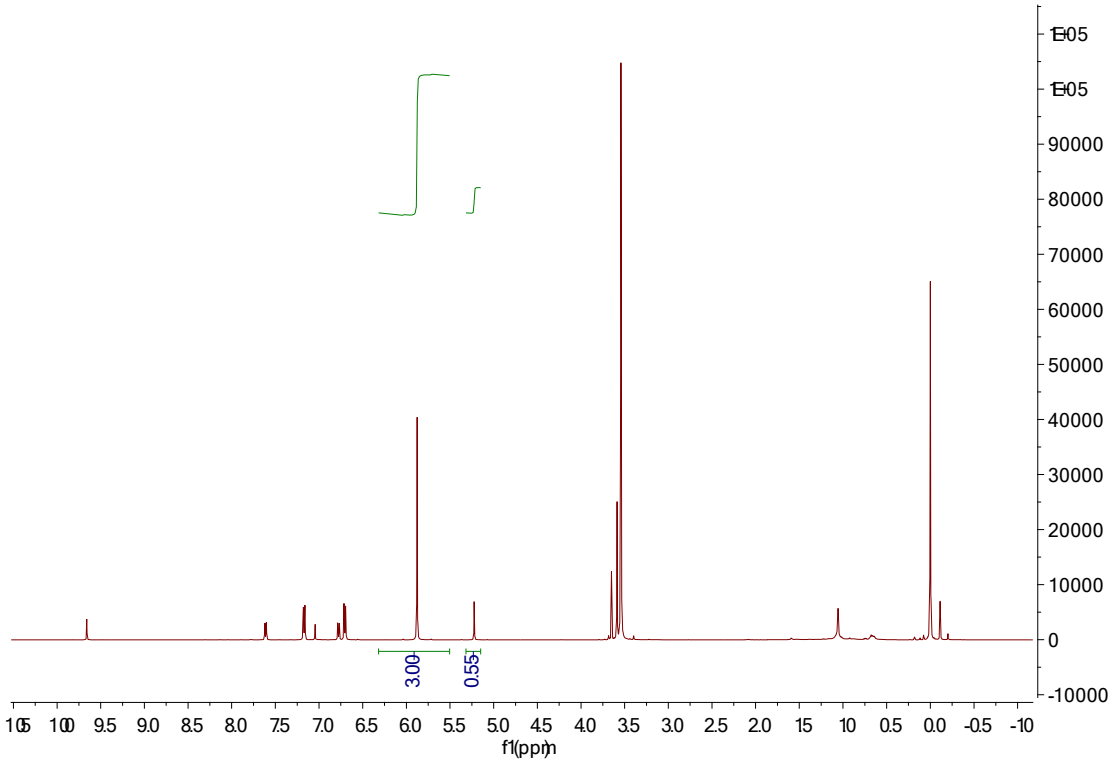

Fig. S62 ^{1}H-NMR for catalysis of 4-methoxybenzaldehyde with in DCM with 2.4 eqv TMSCN for 12h for the forth cycle.
Yiled = 55%

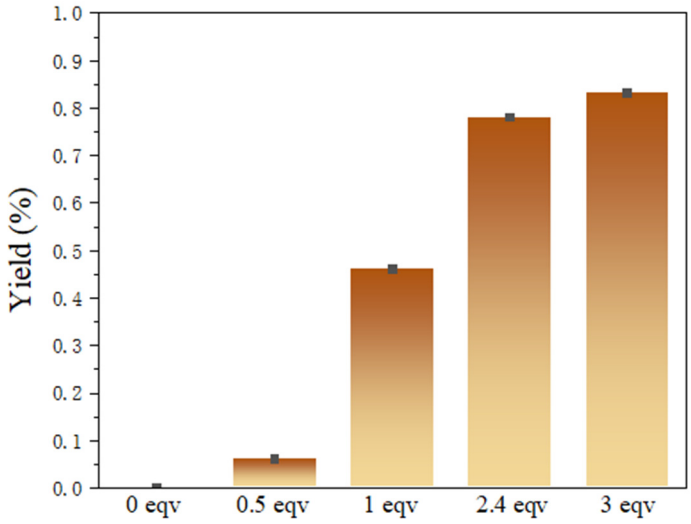

Fig. S63 The yields of cyanosilylation of aldehyde with different amounts of TMSCN (0.5 mmol *p*-methoxybenzaldehyde, 0.01 mmol Tb-MOF, different amounts of TMSCN, in 2 mL DCM at room temperature under Ar condition).
As TMSCN was one of the reactant of the reaction, the amount of TMSCN could affect the yields of the reaction. Consequently, different amounts of TMSCN were added into the reaction and stirred for 12 h. Fig. S63 showed that the yields of 0 equivalent and 0.5 equivalents of TMSCN (compared to the aldehyde) were below 10%, while the yield of 1 equivalent and 2.4 equivalent of TMSCN were about 46%

and 78%, respectively. It was worth nothing that the yield had no significant increase when the amount of TMSCN was 3 equivalent, which encouraged us to choose 2.4 equivalent of TMSCN for further study.

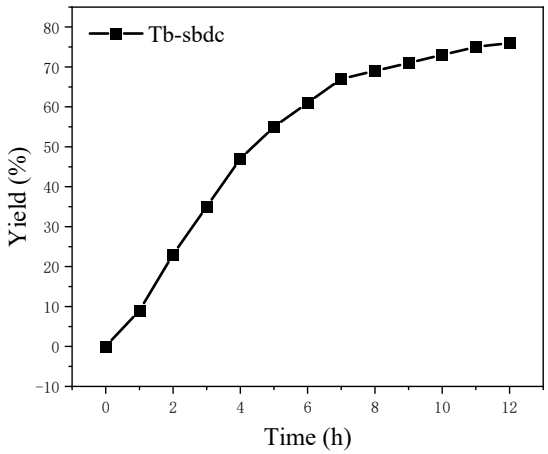

Fig. S64 Catalytic traces of cyanosilylation of *p*-methoxybenzaldehyde with Tb-MOF (0.5 mmol *p*-methoxybenzaldehyde, 1.2 mmol TMSCN, 0.01 mmol Tb-MOF, in 2 mL DCM at room temperature under Ar condition)

To explore the speed of the reaction catalyzed by Tb-MOF, catalytic traces of cyanosilylation was carried out. Fig.S64 showed that the speed of the reaction slowed down after 7 h, and the yield hardly increased after 12 h. Consequently, as the concentration of the substrate getting lower, the speed of the reaction slowed down, which demonstrated that Tb-MOF had an efficient ability for catalyzing cyanosilylation at room temperature. Also, 12 h for the reaction in this condition was enough for further study.

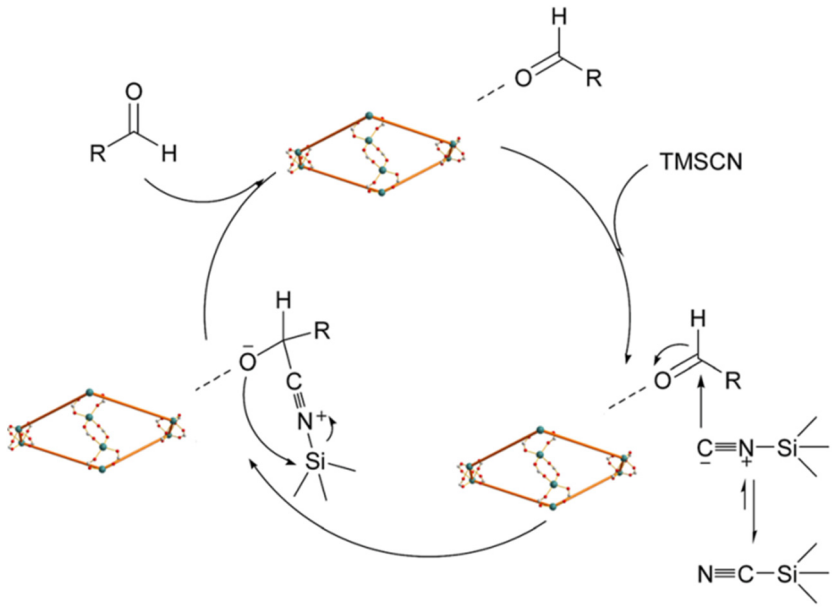

Fig. S65 The possible mechanism of cyanosilylation catalyzed by Tb-MOF.[17]

Table S1 Crystal data and structure refinement for Tb-sbdc.

	Tb-sbdc
Empirical formula	$C_{42}H_{24}O_{21}S_3Tb_2$
Formula weight	1278.63
Wavelength (Å)	0.71073
Crystal size (mm)	0.240×0.220×0.200
Temperature (K)	296 (2)
Crystal system	Triclinic
Space group	*P*-1
a (Å)	13.907 (1)
b (Å)	14.243 (1)
c (Å)	14.994 (1)
α **(deg)**	118.151 (1)
β **(deg)**	99.052 (2)
γ **(deg)**	103.126 (2)
Volume ($Å^3$)	2426.3 (3)
Z	2
Calculated density (Mg/m^3)	1.750
Absorption coefficient **(mm^{-1})**	3.097
F **(000)**	1244
θ **range for data collection (deg)**	1.882 - 25.000
Limiting indices	-16<=h<=16 -16<=k<=16 -17<=l<=17
Reflections collected / unique	52159 / 8540 [R_{int} = 0.0603]
Completeness to **θ = 25.00**	1.00
Data / restraints / parameters	8540 / 0 / 631
Goodness-of-fit on F^2	1.079
Final **R** indices [I>2σ(I)]	R_1 = 0.0337; wR_2 = 0.0882
R **indices (all data)**	R_1 = 0.0462; wR_2 = 0.0928
Largest diff. Peak and hole($e \cdot Å^{-3}$)	1.811 and -0.612

[a] $R_1 = \sum||F_o| - |F_c||/\sum|F_o|$; [b] $wR_2 = [\sum w(|F_o|^2 - |F_c|^2)/\sum w(F_o^2)^2]^{1/2}$; $w = 1/[\sigma^2(F_o^2) + (xP)^2 + yP]$, $P = (F_o^2 + 2F_c^2)/3$.

Table S2 Selected Bond lengths [Å] and angles [deg] for Tb-sbdc.

Tb-sbdc			
Tb(1)-O(3)#1	2.276(4)	Tb(1)-O(19)	2.289(4)
Tb(1)-O(9) #2	2.323(4)	Tb(1)-O(5) #1	2.351(4)
Tb(1)-O(4)	2.374(4)	Tb(1)-O(7)	2.405(4)
Tb(1)-O(11)	2.475(4)	Tb(1)-O(6)	2.513(4)
Tb(2)-O(16)#3	2.260(4)	Tb(2)-O(8)	2.291(4)
Tb(2)-O(10)#2	2.309(4)	Tb(2)-O(15)#4	2.354(4)
Tb(2)-O(14)	2.452(4)	Tb(2)-O(13)	2.481(4)
Tb(2)-O(12)	2.511(4)	Tb(2)-O(11)	2.529(3)
O(11)-Tb(1)-O(6)	120.52(13)	O(3)#1-Tb(1)-O(19)	73.82(15)
O(3)#1-Tb(1)-O(9)#2	141.10(15)	O(19)-Tb(1)-O(9)#2	145.08(15)
O(3) #1-Tb(1)-O(5) #1	75.43(14)	O(19)-Tb(1)-O(5)#1	121.11(15)
O(9)#2-Tb(1)-O(5)#1	78.87(14)	O(3)#1-Tb(1)-O(4)	119.97(14)
O(19)-Tb(1)-O(4)	78.70(14)	O(9)#2-Tb(1)-O(4)	79.93(13)
O(5)#1-Tb(1)-O(4)	75.15(14)	O(3)#1-Tb(1)-O(7)	79.86(14)
O(19)-Tb(1)-O(7)	79.53(15)	O(9)#2-Tb(1)-O(7)	103.31(14)
O(5)#1-Tb(1)-O(7)	140.50(15)	O(4)-Tb(1)-O(7)	144.35(14)
O(3)#1-Tb(1)-O(11)	141.94(13)	O(19)-Tb(1)-O(11)	75.41(13)
O(9)#2-Tb(1)-O(11)	72.42(13)	O(5)#1-Tb(1)-O(11)	141.07(13)
O(4)-Tb(1)-O(11)	74.40(13)	O(7)-Tb(1)-O(11)	72.99(13)
O(3)#1-Tb(1)-O(6)	73.59(15)	O(19) -Tb(1)-O(6)	139.77(15)
O(9)#2-Tb(1)-O(6)	70.84(15)	O(5)#1-Tb(1)-O(6)	71.64(15)
O(4)-Tb(1)-O(6)	139.07(14)	O(7)-Tb(1)-O(6)	72.07(15)
O(12)-Tb(2)-O(11)	51.65(11)	O(16)#3-Tb(2)-O(8)	88.66(16)
O(16)#3-Tb(2)-O(10)#2	145.71(15)	O(8)-Tb(2)-O(10)#2	109.36(15)
O(16)#3-Tb(2)-O(15)#4	103.27(14)	O(8)-Tb(2)-O(15)#4	145.85(14)
O(10)#2-Tb(2)-O(15)#4	78.34(14)	O(16)#3-Tb(2)-O(14)	72.84(15)
O(8)-Tb(2)-O(14)	139.51(14)	O(10)#2-Tb(2)-O(14)	74.77(14)
O(15)#4-Tb(2)-O(14)	74.49(14)	O(16)#3-Tb(2)-O(13)	86.99(14)
O(8)-Tb(2)-O(13)	68.56(14)	O(10)#2-Tb(2)-O(13)	73.81(14)
O(15)#4-Tb(2)-O(13)	142.73(14)	O(14)-Tb(2)-O(13)	74.65(14)
O(16)#3-Tb(2)-O(12)	75.54(13)	O(8)-Tb(2)-O(12)	78.50(13)
O(10)#2-Tb(2)-O(12)	135.38(13)	O(15)#4-Tb(2)-O(12)	73.89(13)
O(14)-Tb(2)-O(12)	127.93(13)	O(13)-Tb(2)-O(12)	142.98(14)
O(16)#3-Tb(2)-O(11)	126.66(13)	O(8)-Tb(2)-O(11)	75.43(13)
O(10)#2-Tb(2)-O(11)	86.83(13)	O(15)#4-Tb(2)-O(11)	71.79(13)
O(14)-Tb(2)-O(11)	144.17(13)	O(13)-Tb(2)-O(11)	129.66(13)

Symmetry transformations used to generate equivalent atoms:

#1: -x, -y+1, -z+1 #2: -x, -y+2, -z+1 #3: x+1, y, z #4: -x, -y+2, -z+2

References

1 Mizuho Y.; Peng L.; Varinia B.; Hirokazu K.; Atsushi F.; Laura G.; Omar F.; Alexander K.; Unprecedented selectivity in molecular recognition of carbohydrates by a metal-organic framework, Chem Commun., 2016, 52, 7094-7097.

2 Tze S.; Tze S.; Warren G.; David Twigg.; Joe C.; David S.; Synthesis of structurally diverse biflavonoids, Tetrahedron, 74 (2018) 5089-5101.

3 Benyamin H.; Maasoumeh J.; Ameneh E.; Abdolreza R.; A Star-Shaped Triazine-Based Vitamin B5 Copper(II) Nanocatalyst for Tandem Aerobic Synthesis of Bis-(indolyl)methanes, Eur. J. Org. Chem., 2020, 4122-4129.

4 Boseok H.; Kim A.; Anna L.; Oxidative C-S Bond Cleavage of Benzyl Thiols Enabled by VisibleLight-Mediated Silver(II) Complexes, Org. Lett., 2020, 22, 4395-4399.

5 Bin Z.; Rui S.; Wan-Min C.; Yao F.; Decarboxylative formylation of aryl halides with glyoxylic acid by merging organophotoredox with palladium catalysis. Org. Chem. Front., 2018, 5, 1782-1786.

6 Seongwoo K.; Jooyeon L.; Sungeun J.; Hoi M.; Min K.; Surface-Deactivated Core-Shell Metal-Organic Framework by Simple Ligand Exchange for Enhanced Size Discrimination in Aerobic Oxidation of Alcohols, Chem. Eur. J., 2020, 26, 7568-7572.

7 Ismail I.; Muhammad I.; Oscar V.; Alireza E.; Peter O.; Håkan E.; Cheuk-Wai T.; Magnus N.; Eric J.; Copper Nanoparticles on Controlled Pore Glass and TEMPO for the Aerobic Oxidation of Alcohols, ChemNanoMat, 2018, 4, 71-75.

8 Wei Z.; Ziqiang X.; Jiajun W.; Wenqin F.; Rong T.; Donghong Y.; Selective Aerobic Oxidation of Alcohols over Gold-Palladium Alloy Catalysts Using Air at Atmospheric Pressure in Water, ChemCatChem, 11, 6, 1779-1788.

9 Ali M.; Reza T.; Reza G.; Design and Fabrication of a Magnetite-based Polymer-supported Hybrid Nanocomposite: A Promising Heterogeneous Catalytic System Utilized in Known Palladium-assisted Coupling Reactions, Combinatorial Chemistry & High Throughput Screening, 23, 2, 119-125.

10 Yujian M.; Ye L.; Yanwei H.; Liang W.; Shilei Z.; Wei W.; Pd-Catalyzed Debenzylation and Deallylation of Ethers and Esters with Sodium Hydride, ACS Catal., 2018, 8, 3016-3020.

11 Siya H.; Meloddy M.; Marcel L.; Sergei R.; Eric H.; Gareth W.; Exploring intermolecular contacts in multisubstituted benzaldehyde derivatives: X-ray, Hirshfeld surface and lattice energy analyses, RSC Adv., 2020, 10, 16861-16874.

12 Babak K.; Leila M.; A Highly Efficient and Recyclable Silica-Based Scandium(III) Interphase Catalyst for Cyanosilylation of Carbonyl Compounds, Org. Lett., 2004, 6, 26.

13 Mahendra S.; Soumen S.; Goutam M.; Gopalan R.; Selvarajan.; A cationic aluminium complex: an efficient mononuclear main-group catalyst for the cyanosilylation of carbonyl compounds, Dalton Trans., 2017, 46, 7672–7676.

14 Jia L.; Ting Y.; Man L.; Qian X.; Weiwei Y.; Li X.; Mengtao M.; Efficient and selective aldehyde cyanosilylation catalyzed by Mg-Libimetallic complex Journal of Organometallic Chemistry, 874 (2018) 83-86.

15 Sandeep Y.; Ruchi D.; Dr. Kumar V.; Dr. Sakya S.; Beyond Hydrofunctionalisation: A Well-Defined Calcium Compound Catalysed Mild and Efficient Carbonyl Cyanosilylation, Chemistry-A European Journal, 24, 6, 1269.

16 Johannes K.; Toni S.; Oliver S.; Athanassios G.; Lewis Acid Mediated Nazarov Cyclization as a Convergent and Enantioselective Entry to *C*-nor-*D*-homo-Steroids, Chemistry-A European Journal, 23，21，5000.

17 Zhiguo Z.; Jingwen C.; Zongbi B.; Ganggang C.; Huabin X.; Qilong R.; Insight into the catalytic properties and applications of metal-organic frameworks in the cyanosilylation of aldehydes, RSC Adv., 2015, 5, 79355-79360.

18 Jan K.; Stefano W.; Thomas.; Kerstin H.; Felix L.; Felix K.; Sandra W.; Franca K.; Steffen B.; Apirat C.; Christophe M.; Bruce H.; Carola B.; Angelo S.; Enrico R.; Matthieu L.; Sylvain F.; Julie R.; Victor H.; Jan H.; Daniel M.; Denys P.; Dieter S.; Stefan K.; Jeremy B.; Ewgenij P.; Discovery of the First in Vivo Active Inhibitors of the Soluble Epoxide Hydrolase Phosphatase Domain, J. Med. Chem., 2019, 62, 8443-8460.

19 Giacomo S,; Daniela L.; Dmitri G.; Ferdinando P.; Ornelio R.; Massimo C.; Luigi V.; Efficient synthesis of cyanohydrin trimethylsilyl ethers via 1,2-chemoselective cyanosilylation of carbonyls Green Chem., 2013, 15, 199-204.

20 Anirban K.; Guilherme R.; Anup P.; Fátima S.; Kamran M.; Firudin C.; Armando P.; Lanthanide metal organic frameworks based on dicarboxyl-functionalized arylhydrazone of barbituric acid: syntheses, structures, luminescence and catalytic cyanosilylation of aldehydes, Dalton Trans., 2017, 46, 8649-8657.

21 Hui Y.; Yongli S.; Zihui X.; Caiyan L.; Kedong Y.; Yi D.; The direct trifluoromethylsilylation and cyanosilylation of aldehydes via an electrochemically induced intramolecular pathway, Chem. Commun., 2020, 56, 2435-2438.

22 Zhi C.; Jian W.; Yanan Z.; Mingqiao G.; Preparation of color tuned highly emissive long-lasting phosphor with warm-toned emitting color based on coating red-emitting coumarin fluorescent dye color converter and PMMA on $SrAl_2O_4:Eu^{2+}$, Dy^{3+} phosphor, Dyes and Pigments, 143 (2017) 190-195.

23 Gurusamy R.; Sung K.; Soney G.; Aluminum phthalocyanine: an active and simple catalyst for cyanosilylation of aldehydes, Applied Organometallic Chemistry, 21, 3, 198-202.